



LUND UNIVERSITY

Quantitative and Qualitative Assessment of the Myocardium at Risk

Ubachs, Joey

2011

[Link to publication](#)

Citation for published version (APA):

Ubachs, J. (2011). *Quantitative and Qualitative Assessment of the Myocardium at Risk*. [Doctoral Thesis (compilation), Clinical Physiology (Lund)]. Department of Clinical Physiology, Lund University.

Total number of authors:

1

General rights

Unless other specific re-use rights are stated the following general rights apply:

Copyright and moral rights for the publications made accessible in the public portal are retained by the authors and/or other copyright owners and it is a condition of accessing publications that users recognise and abide by the legal requirements associated with these rights.

- Users may download and print one copy of any publication from the public portal for the purpose of private study or research.
- You may not further distribute the material or use it for any profit-making activity or commercial gain
- You may freely distribute the URL identifying the publication in the public portal

Read more about Creative commons licenses: <https://creativecommons.org/licenses/>

Take down policy

If you believe that this document breaches copyright please contact us providing details, and we will remove access to the work immediately and investigate your claim.

LUND UNIVERSITY

PO Box 117
221 00 Lund
+46 46-222 00 00

Quantitative and Qualitative Assessment of the Myocardium at Risk

JOEY FA UBACHS, M.D.

DOCTORAL THESIS

which, with due permission from the Faculty of Medicine, Lund
University, will be publicly defended 09:00, Friday, September 2, 2011
Föreläsningssal 3, Skåne University Hospital, Lund



LUND UNIVERSITY

Department of Clinical Physiology
Lund University, Sweden

Faculty opponent

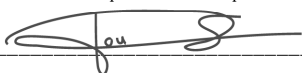
Professor Matthias G Friedrich, M.D.,
University of Calgary, Calgary, Alberta, Canada

Organization LUND UNIVERSITY Department of Clinical Physiology Skåne University Hospital Lund SE-221 85 LUND Sweden	Document name DOCTORAL DISSERTATION	
	Date of issue 2011-07-27	
	Sponsoring organization Swedish Research Council, the Swedish Heart and Lung Foundation, Medical Faculty at Lund University, Sweden and Region of Scania, Sweden.	
Author(s) Joey FA Ubachs		
Title and subtitle Quantitative and Qualitative Assessment of the Myocardium at Risk		
Abstract <p>One of the major determinants of the final infarct size during an acute coronary occlusion is the size of the myocardium subjected to ischemia. Identification and quantification of this so-called myocardium at risk in the acute phase of ischemia has been difficult in patients with conventional methods, such as myocardial perfusion single photon emission computed tomography (SPECT), or electrocardiography. However, to assess cardio-protective strategies aimed at reducing infarct size, an accurate measure of both myocardium at risk and infarct size is needed. Both measurements are necessary in order to assess the amount of myocardium that has been salvaged by the provided treatment. Cardiac magnetic resonance imaging (CMR) has the opportunity to accurately assess both the myocardium at risk as well as the infarct size. This thesis has contributed to the knowledge on myocardium at risk and subsequently myocardial salvage.</p> <p>Paper I demonstrated, for the first time in humans, that there was a good correlation between the myocardium at risk assessed by T2-weighted CMR, which shows myocardial edema, and the myocardium at risk assessed by myocardial perfusion SPECT. Furthermore, the study also showed that T2-weighted CMR can be used up to a week after reperfusion therapy, allowing assessment of both myocardium at risk and infarct size to determine myocardial salvage in a single imaging session, without interfering with patient care.</p> <p>Paper II showed a significant difference between the myocardium at risk assessed by T2-weighted CMR and the endocardial extent of infarction measured by late gadolinium enhancement. Thus, endocardial extent of infarction can not be used to determine myocardium at risk, especially in patients with early reperfusion therapy with little or no infarction.</p> <p>Paper III demonstrated a good correlation between the myocardium at risk assessed by T2-weighted CMR and the myocardium at risk assessed by cine imaging early after injection of a gadolinium-based contrast agent, in patients 1 week after acute coronary occlusion. Thus, both methods can be used simultaneously or separately to determine MaR and subsequently myocardial salvage in a single imaging session.</p> <p>Finally, Paper IV showed that T2-weighted CMR can be used to determine the myocardium at risk in an ex vivo experimental model, both with and without the presence of gadolinium.</p>		
Key words: Acute Myocardial Infarction, Myocardium at Risk, Cardiac Magnetic Resonance Imaging, T2-weighted Imaging, Endocardial Extent of Infarction, Early Gadolinium Enhancement		
Classification system and/or index termes (if any):		
Supplementary bibliographical information:	Language English	
ISSN and key title: 1652-8220	ISBN 978-91-86871-21-5	
Recipient's notes	Number of pages	Price
	Security classification	

Distribution by (name and address)

I, the undersigned, being the copyright owner of the abstract of the above-mentioned dissertation, hereby grant to all reference sources permission to publish and disseminate the abstract of the above-mentioned dissertation.

Signature



Date

2011-07-27

Quantitative and Qualitative Assessment of the Myocardium at Risk

JOEY FA UBACHS, M.D.



LUND UNIVERSITY

Doctoral Thesis
2011

Department of Clinical Physiology
Lund University, Sweden

Cover:

T2-weighted cardiac magnetic resonance image from a patient with an acute coronary occlusion in the right coronary artery. In this short-axis slice, a distinctive bright region can be seen in the inferior wall due to the presence of edema.

ISSN 1652-8220

ISBN 978-91-86871-21-5

Lund University, Faculty of Medicine Doctoral Dissertation Series 2011:71

Department of Clinical Physiology, Lund University
SE-221 85 LUND, Sweden

Printed by: Media-Tryck, Lund University, Sweden

Copyright © 2011 Joey FA Ubachs

Joey.Ubachs@gmail.com

*Patience is the ability to idle your motor,
when you feel like stripping your gears.*

—BARBARA JOHNSON

Contents

List of Publications	ix
Summary	xi
Summary in Swedish / Populärvetenskaplig sammanfattning	xiii
Abbreviations	xv
1 Introduction.....	1
1.1 Ischemic heart disease	1
1.1.1 Pathophysiology	1
1.1.2 Factors influencing development of necrosis	1.1.3
Diagnosis of acute coronary occlusion	6
1.1.3 Diagnosis of acute coronary occlusion	8
1.1.4 Treatment of acute coronary occlusion	9
1.1.5 Assessment of reperfusion strategies	11
1.2 Cardiac imaging techniques	11
1.2.1 Myocardial perfusion single photon emission computed tomography	12
1.2.2 Cardiac magnetic resonance imaging	14
2 Aims of the Work	25
3 Materials and Methods.....	27
3.1 Human studies (Study I, II and III)	27
3.1.1 Study population and design	27
3.1.2 Myocardial perfusion SPECT	28
3.1.3 Cardiac magnetic resonance	29
3.1.4 Statistical analysis	31

3.2	Animal studies (Study IV)	33
3.2.1	Experimental preparation	33
3.2.2	Experimental protocol	34
3.2.3	Myocardial perfusion SPECT	35
3.2.4	Cardiac magnetic resonance	36
3.2.5	Statistical Analysis	38
4	Results and Comments.....	39
4.1	Validation of T2-weighted imaging (Study I)	39
4.2	Endocardial extent of infarction underestimates myocardium at risk (Study II)	43
4.3	Early gadolinium enhancement to assess the myocardium at risk (Study III)	46
4.4	<i>Ex vivo</i> T2-weighted imaging for MaR in the presence of gadolinium (Study IV)	51
5	Conclusions.....	55
	Bibliography	57
	Acknowledgments	69
	Studies I-IV	71

List of Publications

This thesis is based on the following studies, which in the text will be referred to by their roman numerals.

- I. Carlsson M, **Ubachs JFA**, Hedström E, Heiberg E, Jovinge S, Arheden H. Myocardium at risk after acute infarction in humans on cardiac magnetic resonance: quantitative assessment during follow-up and validation with single-photon emission computed tomography. *JACC Cardiovasc Imaging*. 2009; 2(5):569-576.
- II. **Ubachs JFA**, Engblom H, Erlinge D, Jovinge S, Hedström E, Carlsson M, Arheden H. Cardiovascular magnetic resonance of the myocardium at risk in acute reperfused myocardial infarction: comparison of T2-weighted imaging versus the circumferential endocardial extent of late gadolinium enhancement with transmural projection. *J Cardiovasc Magn Reson*. 2010; 12:18.
- III. **Ubachs JFA**, Sörensson P, Engblom H, Carlsson M, Jovinge S, Pernow J, Arheden H. Myocardium at risk by magnetic resonance imaging: head-to-head comparison of T2-weighted imaging and early gadolinium enhanced steady state free precession. *Submitted*.
- IV. **Ubachs JFA**, Engblom H, Koul S, Kanski M, Andersson P, Carlsson M, Erlinge D, Arheden H. Myocardium at risk can be determined by *ex vivo* T2-weighted magnetic resonance imaging even in the presence of gadolinium: comparison to myocardial perfusion SPECT. *Submitted*.

Summary

One of the major determinants of the final infarct size during an acute coronary occlusion is the size of the myocardium subjected to ischemia. Identification and quantification of this so-called myocardium at risk in the acute phase of ischemia has been difficult in patients with conventional methods, such as myocardial perfusion single-photon emission computed tomography (SPECT) or electrocardiography. However, to assess cardioprotective strategies aimed at reducing infarct size, an accurate measure of both myocardium at risk and infarct size is needed. Both measurements are necessary in order to assess the amount of myocardium that has been salvaged by the provided treatment. Cardiac magnetic resonance imaging (CMR) has the opportunity to accurately assess both the myocardium at risk as well as the infarct size. This thesis has contributed to the knowledge on quantification of the myocardium at risk and subsequently myocardial salvage with the use of CMR imaging.

Study I demonstrated, for the first time in humans, that there was a good correlation between the myocardium at risk assessed by T2-weighted CMR, which shows myocardial edema, and the myocardium at risk assessed by myocardial perfusion SPECT. Furthermore, the study also showed that T2-weighted CMR can be used up to 1 week after reperfusion therapy, allowing assessment of both myocardium at risk and infarct size to determine myocardial salvage in a single imaging session, without interfering with patient care.

Study II showed a significant difference between the myocardium at risk assessed by T2-weighted CMR and the endocardial extent of infarction measured by late gadolinium enhancement. Thus, endocardial extent of infarction can not be used to determine myocardium at risk, especially in patients with early reperfusion therapy with little or no infarction.

Study III demonstrated a good correlation between the myocardium at risk assessed by T2-weighted CMR and the myocardium at risk assessed by cine imaging early after injection of a gadolinium-based contrast agent, in patients 1 week after acute coronary occlusion. Thus, both methods can be used simulta-

neously or separately to determine MaR and subsequently myocardial salvage in a single imaging session.

Finally, **Study IV** showed that T2-weighted CMR can be used to determine the myocardium at risk in an *ex vivo* experimental model, both with and without the presence of gadolinium.

Populärvetenskaplig sammanfattning

Under de senaste 10 åren har antalet människor i Sverige som dör av akut hjärtinfarkt minskat stadigt. Den äldre befolkningen är dock växande och med ökande antal människor med fetma och typ II-diabetes, står vi inför en stor utmaning i framtiden vad gäller hantering av patienter med akut hjärtinfarkt. För att möta denna utmaning är det viktigt att öka vår förmåga att behandla akut hjärtinfarkt. Korrekt behandling har dock alltid förlitat sig på korrekt diagnos. Ökad noggrannhet och precision av diagnostisk prestanda är därför viktigt, inte bara för den enskilda patienten men också för samhället, eftersom en liten behandlingsvinst kan ge stora besparingar på grund av det stora antalet patienter. Identifiering och kvantifiering av det ischemiska område, även kallat för riskarea, i den akuta fasen av ischemi har varit svårt på patienter med konventionella metoder, t.ex. scintigrafi eller elektrokardiogram. Om man vill undersöka nya behandlingsstrategier, med syfte att reducera infarktstorlek, behövs tillförlitliga mått på både infarktstorlek och riskarea för att kunna bedöma hur mycket som räddas med hjälp av olika behandlingsstrategier. Denna avhandling har i stor grad ökat kunskapen kring möjligheten att kunna bestämma riskarea med hjälp av magnetresonancetomografi (MR).

Delarbete I visade för första gången i människa att riskarea med T2-viktad MR, vilket visar ödem i hjärtmuskeln, korrelerade med scintigrafi (referensmetod för bestämning av riskarea). Studien visade även att T2-viktad MR kan användas för bestämning av riskarea upp till en vecka efter reperfusionsbehandling. Vid jämförelse med infarktstorlek sågs att stora delar av riskarean hade räddats genom reperfusionbehandling.

I **delarbete II** undersöktes sambandet mellan riskarea mätt med T2-viktad MR och den endokardiella utbredningen av infarktstorlek mätt med kontrastförstärkt MR. Studien visade en signifikant skillnad mellan dessa två metoder för att bestämma riskarea. Studien visade att den endokardiella utbredningen av

infarkt kan inte användas för att bestämma riskarea hos patienter med tidig reperfusionsbehandling med liten eller ingen infarkt som följd.

I **delarbete III** studerades hur riskarea vid reperfunderad förstagångsinfarkt mätt med T2-viktad MR förhåller sig till riskarea mätt med funktionsbilder tidigt efter kontrastinjektion (EGE). Studien visade ett starkt samband mellan de två olika metoderna för att bedöma riskarea. Slutsatsen från denna studie är att både T2-viktad MR och EGE kan användas för att bedöma riskarea och räddad hjärtmuskel.

Delarbete IV visade att T2-viktad MR i en ex vivo modell i gris kan användas för att bedöma riskarea. Dessutom studerades om T2-viktad MR kan användas för att bedöma riskarea efter injektion av MR-kontrastmedel innehållande gadolinium. Resultaten visade att riskarea på T2-viktade bilder, med och utan kontrast, korrelerade starkt med scintigrafi.

Abbreviations

Ao	aorta
ATP	adenosine triphosphate
B	main magnetic field
^{11}C	carbon
Ca^{2+}	calcium
CABG	coronary artery bypass grafting
CK-MB	creatine kinase isoenzyme MB
CMR	cardiac magnetic resonance
CT	computed tomography
ECG	electrocardiography
EGE	early gadolinium enhancement
Gf	frequency encoding gradient
Gp	phase encoding gradient
Gs	slice selective gradient
^1H or H^+	hydrogen
K^+	potassium
KeV	kilo-electronvolt
LA	left atrium
LAD	left anterior descending artery
LCx	left circumflex artery
LGE	late gadolinium enhancement
LV	left ventricle
M	net magnetization
MaR	myocardium at risk
MBq	megabecquerel
MI	myocardial infarction
MLEM	maximum likelihood-expectation maximization
MR	magnetresonanstomografi
MRI	magnetic resonance imaging
mSv	millisievert

^{23}Na or Na^+	sodium
^{31}P	fosfor
PCI	percutaneous coronary intervention
PET	positron emission tomography
RA	right atrium
RCA	right coronary artery
RF	radio frequency
ROS	reactive oxygen species
RV	right ventricle
SD	standard deviation
SPECT	single-photon emission computed tomography
SSFP	steady state free precession
STEMI	ST-elevation myocardial infarction
STIR	short TI inversion-recovery
T	tesla
T2-STIR	T2-weighted triple inversion-recovery sequence
T2-TSE	T2-weighted double inversion-recovery sequence
$^{99\text{m}}\text{Tc}$	technetium
TE	echo time
TI	inversion time
TIMI	trombolysis in myocardial infarction
TR	repetition time
TTC	triphenyltetrazolium chloride

Chapter 1

Introduction

1.1 Ischemic heart disease

Ischemic heart disease is the leading cause of morbidity and mortality in the western world. The number of patients who developed an acute coronary syndrome has been increasing exponentially, and in 2007 it was estimated that approximately 400.000 Americans died of an acute coronary occlusion. Furthermore, each year approximately 785.000 Americans suffer from a new coronary occlusion. This means that every 25 seconds a new coronary event will occur, and approximately every minute, someone will die of one.¹ In Sweden, the number of people that died from an acute coronary occlusion has declined by 27% over the last 10 year. However, still 10.000 people die each year and it is therefore still considered the single most important cause of death in Sweden.²

Notwithstanding the decline over the last 10 years, the elderly population is growing, and with the increasing number of people with obesity and subsequently type-2 diabetes, we are facing an even bigger challenge in the future handling patients with acute coronary occlusion. To face this challenge, it is important to gain insight into the pathophysiology and increase our ability to treat acute coronary occlusion. Correct treatment, however, has always relied on accurate diagnosis. Enhancing the accuracy and precision of diagnostic performance is therefore important, not only for the individual patient but also for society, since a small benefit in outcome may yield major savings.

1.1.1 Pathophysiology

Ischemic heart disease evolves from a disease in the coronary arteries, most commonly atherosclerosis. The coronary arteries are conductance vessels; their

principal role is to deliver oxygen-rich blood to the myocardium so it can maintain its function. In a normal heart, the coronary arteries provide almost no resistance to blood flow, and myocardial circulation is mainly controlled by constriction and dilation of arterioles in the myocardium. In advanced atherosclerosis, the coronary artery can be partly blocked by an atherosclerotic plaque, which decreases the blood pressure distal to the sclerotic zone. To compensate for this reduced blood pressure, coronary arteries will dilate to maintain normal resting blood flow. Thus, most patients with coronary atherosclerosis do not have symptoms of ischemia at rest, depending of course on the extent of the stenosis of the coronary artery.³ During exercise, however, the capacity of the coronary arteries to dilate further is limited, and subsequently, there is a decreased blood flow reserve. As a result, there is a higher demand of oxygen-rich blood during exercise that can no longer be delivered by the coronary arteries. Hence, when the coronary arteries can not deliver enough oxygen-rich blood to supply the myocardial demands, myocardial ischemia occurs.

Although myocardial ischemia often occurs during physical activity, myocardial ischemia can even occur at rest. In advanced atherosclerosis, the atherosclerotic plaque in the coronary artery is very vulnerable to rupture, and when this occurs, substances within the plaque are exposed to the blood promoting thrombosis, thereby occluding the coronary artery.

If the coronary occlusion is not directly treated, and coronary blood flow is not restored, a series of events can occur, either simultaneously or sequential.⁴ The numbers of each section described below correspond to the numbers seen in Figure 1.1.

1. Interruption of blood supply decreases delivery of oxygen and glucose.

2. Metabolic shift

When tissues are deprived from oxygen, the energy-rich adenosine triphosphate (ATP) can no longer be produced by aerobic glycolysis. Instead, the metabolism shifts from aerobic to anaerobic and the end-product pyruvate is reduced to lactate in the cell, where its accumulation lowers the cellular pH. A decreased pH results in a decreased activity of many cellular enzymes that are necessary to maintain normal function.

3. Ionic imbalance

Distortion of the activities of pumps in the plasma membrane changes the ionic balance of the cell. The lack of ATP results into an inactive Na^+/K^+ -pump, which causes sodium to accumulate intracellularly and

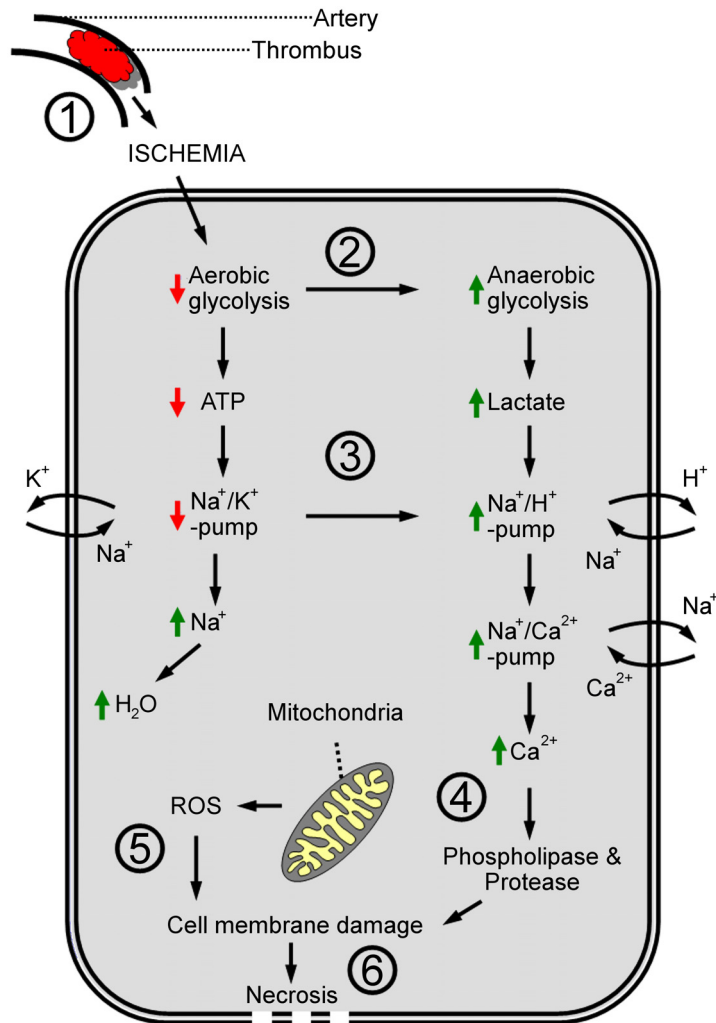


FIGURE 1.1 Schematic overview of the ischemic cascade in the cell. The numbers 1-6 correspond to the numbers 1-6 in section 1.1.1 Pathophysiology. ATP = adenosine triphosphate; ROS = reactive oxygen species.

potassium to diffuse out of the cell. This gain of sodium is accompanied by the influx of water, causing the cell to swell. The failure of the Na^+/K^+ -pump leads to activation of the Na^+/H^+ -pump. This pump is normally dormant, but when intracellular acidosis threatens, H^+ is pumped out of the cell in exchange for Na^+ , to maintain normal pH. The resulting increase in intracellular sodium activates the $\text{Na}^+/\text{Ca}^{2+}$ -pump, causing calcium to flow into the cell in exchange for sodium. Normally, excess intracellular Ca^{2+} is forced out of the cell by an ATP dependent calcium pump. However, since only a limited amount of ATP is available, Ca^{2+} will accumulate in the cell.

4. Phospholipase and protease activation

High calcium concentrations inside the cell activate phospholipase A2, leading to degradation of membrane phospholipids and consequent release of free fatty acids and lysophospholipids. The latter acts as a detergent that disrupts the cell membrane.⁵⁻⁷ Furthermore, fatty acids and lysophospholipids are potent mediators of inflammation, an effect that may further disrupt the integrity of the already compromised cell.

Calcium also activates a series of proteases that attack the cytoskeleton and its attachments to the cell membrane.⁵ As the cohesion between cytoskeletal proteins and the plasma membrane is disrupted, membrane blebs form, and the shape of the cell is altered.

5. Reactive oxygen species

Cells also generate energy by reducing oxygen to water. During this process, small amounts of partially reduced oxygen are produced as an unavoidable by-product of mitochondrial respiration. Some of these forms are free radicals that can damage lipids, proteins and nucleic acid. They are referred to as reactive oxygen species (ROS).⁸ Under normal circumstances, about 2% of the oxygen is converted to ROS and our natural defense system can prevent injury from happening. During ischemia, an imbalance occurs, which can result in oxidative stress, a condition that has been associated with cell membrane injury.⁹

6. Transition from reversible to irreversible injury

In myocardial ischemia, there is no striking sudden change that marks the point of transition from viable myocardium to irreversible injured myocardium. Up till now, the cell is reversibly damaged, and myocardial function can be recovered given that blood flow is restored.

However, when the duration of ischemia is prolonged, the cell can no longer maintain itself as a metabolic unit and it becomes irreversibly damaged, necrotic cell death will occur. At this point, two distinctive changes can be seen in the cell: the presence of amorphous matrix densities in mitochondria and loss of cell membrane integrity. The development of necrotic cell death is species dependent and will be discussed later in this thesis.

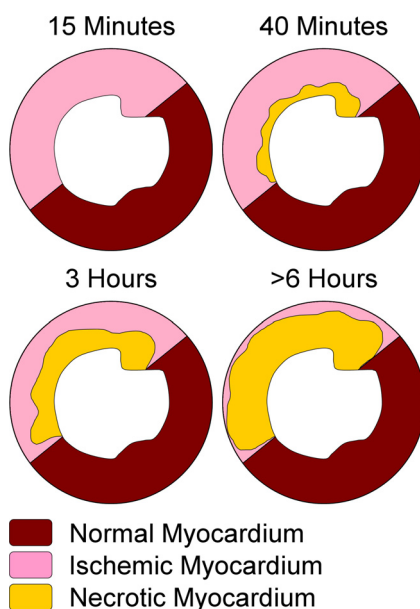


FIGURE 1.2 Schematic short-axis slices of the left ventricle of the heart with an occlusion in the left anterior descending coronary artery. With increasing duration of ischemia, myocardial necrosis (yellow) will evolve within the ischemic myocardium (pink) in a wavefront manner from the endocardial borders of the myocardium towards the epicardium, a concept first demonstrated in a dog model by Reimer *et al.* in 1977.¹¹

1.1.2 Factors influencing development of necrosis

Duration of ischemia. A major determinant that affects the transition from reversible to irreversible injured myocardium is the duration of ischemia.¹⁰ With increasing duration of ischemia, myocardial necrosis will evolve within the myocardium supplied by the occluded vessel in a wavefront manner from the endocardium towards the epicardium (Figure 1.2).¹¹ If there is no restoration of blood flow, necrosis will ultimately involve the full thickness of the myocardial muscle wall, a so called transmural myocardial infarction. On the positive side, if blood flow is restored within a certain time period, there will not be a development of myocardial necrosis,^{12, 13} which is called aborted infarction.^{14, 15}

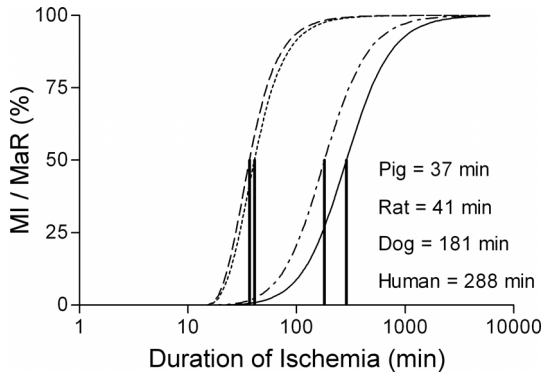


FIGURE 1.3 Infarct progression for different species. The indicated minutes are the times to reach 50% myocardial infarction of the initial ischemic myocardium. There was a significantly slower infarct evolution in man compared to pigs, rats and dogs. (Reprinted with permission from Hedström *et al.*)¹⁶

Whereas the time course of infarct evolution is well known in animals due to controlled experiments, in humans, this is much more challenging. Recently, Hedström *et al.*¹⁶ provided evidence of infarct evolution in humans in relation to the initial ischemic region. Their results showed that approximately 50% of the ischemic myocardium has become irreversibly injured after almost 5 hours of occlusion (Figure 1.3). Furthermore, infarct evolution in humans showed to be significantly slower than infarct evolution in pigs, rats and dogs. Thus, with

time, acute ischemic heart disease leads by necessity to transmural infarction unless the acute event is treated by reperfusion therapy in time.^{17, 18} The current guidelines state that the treatment focus should be on increasing the number of patients with timely access to percutaneous coronary intervention (PCI). This focus should not only be on limiting the time from pain onset to arrival at the hospital, but also on limiting the time from arrival at the hospital to reperfusion.¹⁹ It was recently shown that a delay in time to reperfusion after arrival at the hospital was associated with a higher risk of in-hospital mortality up to 10.3%.²⁰

Preconditioning. Some patients may arrive at the emergency department with complaints of on-and-off chest pain over a period of hours or even days. In these patients, the myocardium has been subjected to repetitive short ischemic episodes. Due to these repetitive ischemic episodes, the myocardium has increased its tolerance for ischemia and when total occlusion finally occurs, the myocardium is able to survive longer before becoming irreversibly injured. This phenomenon is called ischemic preconditioning,²¹ and there is a general agreement that other than early reperfusion, preconditioning is a potent form of *in vivo* protection against ischemic myocardial injury. Ischemic preconditioning has been shown to consistently reduce myocardial infarct size experimentally in dogs, rats, rabbits and pigs.²¹⁻²⁵ Data from clinical studies suggest that preconditioning also occurs in humans.^{26, 27}

The mechanisms for preconditioning are complicated and not fully understood. They seem to involve a variety of stress signals which include activation of membrane receptors and signaling molecules.²⁸ They also involve a much lower utilization of ATP as well a lower accumulation of lactate in preconditioned myocardium compared to the non-preconditioned myocardium.^{26, 29} This suggests that preconditioned myocardium has a reduced energy demand and consequently a delayed onset of necrosis when blood flow is interrupted. As a result, a slower progression of necrosis implies a longer window of time in which it may be possible to salvage myocardium by reperfusion therapy.

Collateral flow. A third factor, influencing the extent of ischemia as well as the extent of irreversibly injured myocardium, is the presence and degree of collateral vessels. Collateral vessels are defined as small vessels that interconnect coronary arteries. They exist latently in the normal heart, although their presence varies between species.^{30, 31} In response to myocardial stress factors, these microscopic collateral vessels undergo a process called transformation that widens the lumen of the vessels. Consequently, the collateral vessels may deliver

sufficient blood and may slow cellular injury to allow survival of at least part of the initial ischemic region when the coronary artery is suddenly occluded. The myocardial stress factors that influence this transformation can be: myocardial spasms, inflammation, shear stress or lack of oxygen. The latter being probably the most important one in coronary artery disease. To point out the importance of collateral vessels; guinea pigs do not produce myocardial infarction at all when a single coronary artery is occluded due to their very well developed intracoronary collateral network, which maintains normal perfusion.³⁰

In humans with acute coronary occlusion and no previous history of coronary heart disease, sufficient collateral vessels to maintain normal perfusion of the myocardium may not have been developed yet due to the absence of myocardial stress factors. However, in patients with severe angina pectoris, well developed collaterals can be seen.³² Furthermore, patients with collateral vessels have a smaller infarct size, less depressed left ventricular function and better survival rates than patients without collateral vessels.^{33, 34}

Size of the ischemic region. Apart from duration of ischemia, collateralization and preconditioning, a major determinant of final myocardial infarction is the size of the myocardium subjected to ischemia.^{35, 36} The size of ischemia depends on the coronary distribution as well as the location of the occlusion in the coronary arterial bed.³⁷ This implicates that two patients with the same infarct size do not necessarily need to have the same size of ischemia, and hence, this shows how important an accurate measure of the ischemic region is when assessing outcome of new reperfusion strategies. Furthermore, the ischemic region has stopped functioning due to the altered metabolism during ischemia, a process called stunning.³⁸ Myocardial stunning remains present up to several weeks after the coronary artery has been opened, and an important clinical implication of stunning is that this phenomenon may contribute to heart failure, depending on the extent of the myocardium that is stunned.

1.1.3 Diagnosis of acute coronary occlusion

First, a clear distinction should be made between the terms myocardial infarction and myocardial ischemia. The term myocardial infarction reflects cell death of cardiac myocytes caused by ischemia, which is the result of an imbalance between blood supply and demand. The term myocardial infarction should therefore only be used when there is evidence of necrosis, in relation to the circumstances leading to the infarct (e.g. spontaneous or procedure related), and in relation to the timing of the infarct relative to the time of the observation (evolving, healing, or healed myocardial infarction).³⁹

Clinical signs of ischemia can most often be identified from the patients' history. Possible symptoms include various combinations of chest, upper extremity, jaw, or epigastric discomfort during exercise or at rest, and may be accompanied by shortness of breath, sweating, nausea or loss of consciousness. These symptoms, however, are not specific to myocardial ischemia and can be misdiagnosed. Myocardial ischemia may even occur with atypical symptoms, or even without symptoms. Therefore, acute myocardial ischemia/infarction is defined as a combination of at least two of the following criteria: 1) typical symptoms of ischemia, 2) acute electrocardiographic changes including ST-segment deviation, T-wave elevation, new left bundle branch block or Q-wave development, 3) detection of rise and/or fall of cardiac biomarkers, preferably troponin, and 4) imaging evidence of new loss of viable myocardium or new regional wall motion abnormalities.³⁹

Patients with complaints of chest pain but no further signs of acute coronary occlusion can be subjected to either cardiac exercise testing,⁴⁰ myocardial perfusion single-photon emission computed tomography (SPECT) with or without pharmacological stress induction,⁴¹ or perfusion cardiac magnetic resonance (CMR) imaging after injection of dobutamine,⁴² to assess whether there is an exercise-induced ischemia and whether they would benefit from treatment.

1.1.4 Treatment of acute coronary occlusion

When a patient shows signs of an acute coronary occlusion, the main goal of treatment is to restore blood flow to the ischemic myocardium to minimize the extent of myocardial infarction. Even though blood flow is spontaneously restored in some patients through activation of the fibrinolytic system, pharmacological and more so mechanical reperfusion can be of great value.^{43, 44} Current clinical guidelines recommend that patients with signs of acute coronary occlusion undergo PCI within 90 minutes.¹⁹ However, in more remote regions, hospitals may not be able to perform these procedures, and pharmacological reperfusion might therefore be more appropriate at these hospitals. In Figure 1.4 a schematic overview of possible treatment strategies is given according to the current guidelines.¹⁹

The aim of pharmacological reperfusion in the acute phase is to promote the fibrinolytic system to dissolve the occluding thrombus and to prevent further thrombus growth that occurs through platelet inhibition and anticoagulation. Although studies have shown the benefits of pharmacological reperfusion,⁴⁵ a major limitation is that it is not possible to directly assess whether blood flow has been fully restored in the ischemic myocardium.

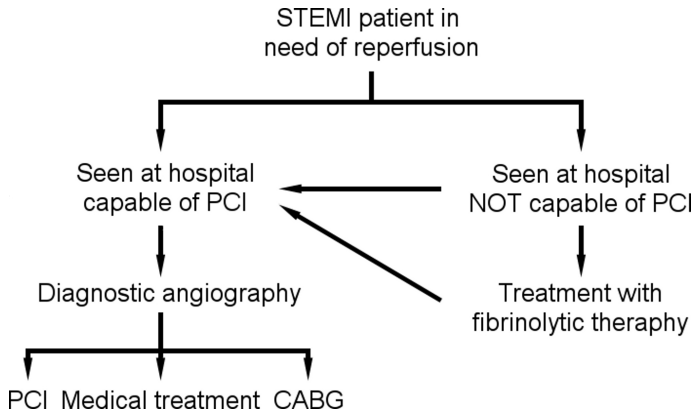


FIGURE 1.4 Schematic overview of possible treatment strategies for patients with ST-elevation myocardial infarction (STEMI), according to the current guidelines. Patients seen at a hospital not capable of percutaneous coronary intervention (PCI) may be transferred to a PCI capable hospital if the patient would benefit more from mechanical reperfusion. Those patients treated with fibrinolytic therapy, where ischemic symptoms persist and failure to reperfuse is suspected, may also be transferred. CABG: coronary artery bypass grafting. (Adapted from Kushner *et al.*)¹⁹

Mechanical reperfusion is most often achieved by PCI, where a balloon is inflated at the location of the occlusion. Thereafter, a stent is expanded into the vessel wall to prevent reoccurrence of the occlusion. In those patients not suitable for PCI or with multivessel disease, mechanical reperfusion can be achieved by coronary artery bypass grafting (CABG).^{46, 47} During this procedure an artery or a vein from elsewhere in the patient's body is grafted to the coronary arteries to bypass the atherosclerotic occlusion.

In addition to restoration of coronary blood flow, myocardial infarct mortality has been reduced throughout the years by introducing specialized coronary care units, and drugs such as thrombocyte aggregation inhibitors, angiotensin-converting enzyme inhibitors, beta receptor inhibitors, and statins.⁴⁸

Coronary heart disease is a chronic condition, and patients who have recovered from an acute coronary occlusion are at high risk for new events and premature death. Approximately 10% of post-infarction patients have a

recurrent occlusion within one year after discharge,⁴⁹ and mortality after discharge remains much higher than in the general population. Therefore, possible causes of coronary heart disease should be discussed with the patient during hospitalization, and advice on a healthy diet, weight control, smoking and exercise should be given.

1.1.5 Assessment of reperfusion strategies

As mentioned above, acute occlusion of a coronary artery initiates a progressive process of necrosis from the endocardium to the epicardium over time, the so-called wavefront phenomenon. Without reperfusion or collateral flow from other arteries, this process ends in complete necrosis of the region supplied by the occluded vessel. To assess the efficiency of reperfusion therapy, two important measurements should be obtained. First, an accurate measure of the size of the ischemic region behind the occlusion should be acquired. This ischemic region is referred to as the **myocardium at risk (MaR)** throughout the remainder of this thesis. Secondly, an accurate measure of the size of irreversibly injured myocardium should be obtained, called **myocardial infarction (MI)**. Finally, the efficiency of reperfusion therapy can be assessed by studying the relation between myocardium at risk and final infarct size. This relation is called **myocardial salvage** and expresses how much of the initial myocardium at risk has been saved by reperfusion therapy. How myocardial salvage can be calculated will be discussed in Chapter 3.

1.2 Cardiac imaging techniques

There are a number of techniques that have the possibility to generate images of the heart. These techniques depend on different principles of physics on how the images are generated. More importantly, different techniques can visualize different characteristics, such as cardiac anatomy, physiology, function or a combination of these. It is therefore important to consider the advantages and limitations of each technique before choosing a technique to visualize the different characteristics of the heart.⁵⁰ Potential imaging techniques include echocardiography, X-ray, computer tomography (CT), positron emission tomography (PET), myocardial perfusion single-photon emission computed tomography (SPECT) and magnetic resonance imaging (MRI). This thesis is not meant to give a detailed description of all the potential techniques, and the following sections will therefore only focus on those techniques used in this thesis.

1.2.1 Myocardial perfusion single photon emission computed tomography

Myocardial perfusion SPECT is a widely utilized nuclear medicine imaging technique for the diagnosis of coronary artery disease after injection of a radioactive tracer and subsequent imaging with a gamma camera. Myocardial perfusion SPECT can be performed at rest or during exercise and can detect, localize, and quantify the degree of ischemic myocardium. The result of a myocardial perfusion SPECT is related to the prognostic outcome of cardiac events. Therefore, myocardial perfusion SPECT is used to guide treatment in patients with stable angina and after acute coronary occlusion. Myocardial perfusion SPECT is a mature technique and part of the international guidelines for treatment of patients with ischemic heart disease.^{48, 51, 52} There are international guidelines on how to perform, how to report and when to use myocardial perfusion SPECT.^{41, 53, 54}

Myocardial perfusion SPECT has shown to correlate well with the myocardium at risk when the radioactive tracer is injected during occlusion before opening of the coronary artery.^{55, 56} When the radioactive tracer is injected after opening of the coronary artery, the perfusion defect seen on the images is more likely to correlate with myocardial infarct size.⁵⁷

Radioactive tracers

Cardiac nuclear medicine studies are based on the injection of a gamma-emitting radioactive tracer, which is distributed in relation to perfusion. Image quality depends heavily on the physical properties of this radioactive tracer and preferably, a good tracer requires: a high grade of extraction from blood, preferential uptake into cardiac myocytes, a rapid decay to make a repeat examination possible, and a distribution proportional to regional blood flow. The most commonly used perfusion tracers are technetium 99m (^{99m}Tc)-labeled tetrofosmin or sestamibi, which have a superior image quality compared to the formerly used tracer thallium-201 due to their higher emission of energy.⁵⁸ The photons from the technetium-labeled tracers are emitted at approximately 140 keV, which is well suited for gamma camera imaging, and which results in less photon attenuation and scatter due to soft tissue as compared to thallium-201, where the photons are emitted at approximately 82 keV.

Thallium has a rather long half-life of 73 hours, and the radiation dose is somewhat high (18 mSv), which makes this tracer less favorable to use in patients. Thallium can be found in the same group as potassium in the periodic

table and it has therefore a similar biological behavior. Thallium enters myocytes by both active transport and passive diffusion, and is distributed fast into the myocardium in proportion to the blood flow. Following thallium's initial extraction, there is a continuous exchange between the myocytes and the extracellular compartment, resulting in a phenomenon known as redistribution. Intake of thallium into the cell continues via additional extraction of thallium that still remained in the blood and via extraction of thallium that re-circulated after it has been washed out of the intracellular compartment. Redistribution often begins as early as 20 minutes following thallium administration,⁵⁹ and may result in the partial or total resolution of perfusion defects noted shortly after stress imaging. Therefore, imaging has to be performed within 10-15 minutes after administration to be able to visualize any perfusion defects.

^{99m}Tc has good characteristics for myocardial perfusion SPECT acquisitions, with a medium half-life of approximately 6 hours and a relatively low radiation dose for a combined rest and stress study (7-8 mSv). The extraction of tetrofosmin and sestamibi from the blood is slower than thallium and they diffuse passively into the myocytes. Once the tracers are in the myocytes, they are bound to the mitochondria and can only be cleared metabolically. Consequently, the injection does not have to be adjacent to the gamma camera, and the patient can be transported to the gamma camera without haste. However, this also means that a separate resting injection must be administered if stress imaging shows a perfusion defect.

Image acquisition

To acquire perfusion images, a gamma camera is used to detect the radiation emitted from the tracer injected into the patient. The gamma camera normally consists of one or more detectors that detect the emitted radiation. These detectors are equipped with a filter, a collimator, which only detects photons that hit the detector at a 90 degree angle. Thus, rotation around the body is necessary to acquire data covering the entire heart. A typical myocardial perfusion SPECT acquisition uses 2 detectors with a rotation arc of 90 degrees. The detectors acquire data during a certain time and then move to the next predefined position along its orbital path. When a photon is finally absorbed into one of the detectors, scintillation occurs and the created light spot is registered by photomultiplier tubes, amplified, and sent through decoding circuits that record the energy and spatial location of the photon.

Once image acquisition has been performed at all angles, the data is reconstructed to enable assessment of left ventricular volumes and myocardial perfusion.

Limitations

Radiation originating from different parts of the myocardium travels different distances through the chest towards the gamma camera detector. If there is tissue of high density between the myocardium and the detector, some photons may not reach the detector. This is called attenuation of the signal and may mimic a perfusion defect in both rest and stress myocardial perfusion SPECT images.⁶⁰ Additional imaging in the prone position or transmission attenuation correction can be used to overcome this problem. Today, hybrid systems combining myocardial perfusion SPECT with CT are available, and the information gained from CT can be used for attenuation correction.⁶¹ Furthermore, myocardial perfusion SPECT has a limited spatial resolution, affecting its ability to detect non-transmural perfusion defects. Due to this limited spatial resolution, it is also difficult to distinguish papillary muscles that are often excluded when analyzing the myocardium by MRI. Finally, in instances where there is a large perfusion defect present within the apical regions of the myocardium, it can be difficult to accurately assess the size of the left ventricle, which may potentially affect the quantification of the ischemic area. Commercially available algorithms exist for segmentation of the LV in myocardial perfusion SPECT,^{62, 63} which showed to underestimate the LV mass compared with manual segmentation of MRI images.⁶⁴ More recently, an algorithm was developed by Soneson *et al.*⁶⁵ for automatic delineation of LV volumes based on MRI data in patients where a perfusion defect was present on the myocardial perfusion SPECT images.

1.2.2 Cardiac magnetic resonance imaging

In this section, the basic principles of magnetic resonance imaging will be introduced. The descriptions are not meant to be exhaustive, and since many principles are quite complex, explanations are kept as simple as possible focusing only on those that are important for this thesis. More detailed information on MRI can be found elsewhere.⁶⁶⁻⁶⁸

An MRI system has three main components necessary for generating images: the main magnet, three gradient coils and a radiofrequency coil. The first two are built into the MRI unit, while the radiofrequency (RF) coil can be selected by the operator depending on the anatomy to be examined. These components each generate a different type of magnetic field, which in combination produces spatial information of magnetic resonance signals. Finally, a fourth component is necessary, a computer system, which is the core unit for the instructions and control of all the components in the scanner. In addition, the computer is used to process all the magnetic resonance signals to compose the final MR image.

Basic Principles

There are a number of elements, including ^{31}P , ^{23}Na and ^{13}C , whose nuclei exhibit properties that can be used for magnetic resonance imaging. However, hydrogen (^1H) is generally used to create MR images due to its natural abundance in the form of water and lipid molecules. Hydrogen consists of a single proton, which has a magnetic moment. This magnetic moment has a magnitude and a direction. The magnitude is identical for all protons, but the orientation is random (Figure 1.5a). Once placed in an external magnetic field (B_0), such as an MRI system, the magnetic moments start to spin (precess) around the direction of the magnetic field (B_0) (Figure 1.5b). The frequency of precession is determined by the strength of the magnetic field and the type of nucleus, and is called the Larmor frequency. The precessions are not in phase at this point in time. The magnetic moments interact with each other and the magnetic field. As a result, they slowly find an equilibrium state where a small fraction of the magnetic moments are aligned along the applied magnetic field (B_0) (Figure 1.5b). A slightly larger fraction of the magnetic moments will be aligned with the magnetic field since this requires the least amount of energy. The fraction of protons that are aligned with the applied magnetic field is directly related to the strength of the magnetic field and the temperature. The sum of all the magnetic moments combined form a net magnetization (M_0), which also precesses around the magnetic field. The magnitude of the net magnetization (M_0) determines the maximal signal intensity that can be generated and used to form images. Thus, the greater the applied magnetic field strength (B_0), the greater the amount of magnetic moments aligned with the magnetic field and the greater the size of the net magnetization (M_0). A typical field strength used for cardiac imaging is 1.5 Tesla, which is approximately 30,000 times stronger than the earth's magnetic field strength.

Radio frequency

In order to generate a MR signal from the net magnetization, the magnetization has to be deviated from its equilibrium state. This is achieved by letting the system absorb energy. Energy is supplied via generation of a radiofrequency (RF) field, applied at a characteristic Larmor frequency and at an angle orthogonal to the main magnetic field (B_0). The RF field is normally generated by a short pulse from the RF coils. When the RF pulse is switched on, two effects will occur: some protons are lifted to a higher level of energy and align against the main magnetic field, and it also causes the protons to precess in phase (Figure 1.5c). The net magnetization (M_0) begins to rotate away from its alignment.

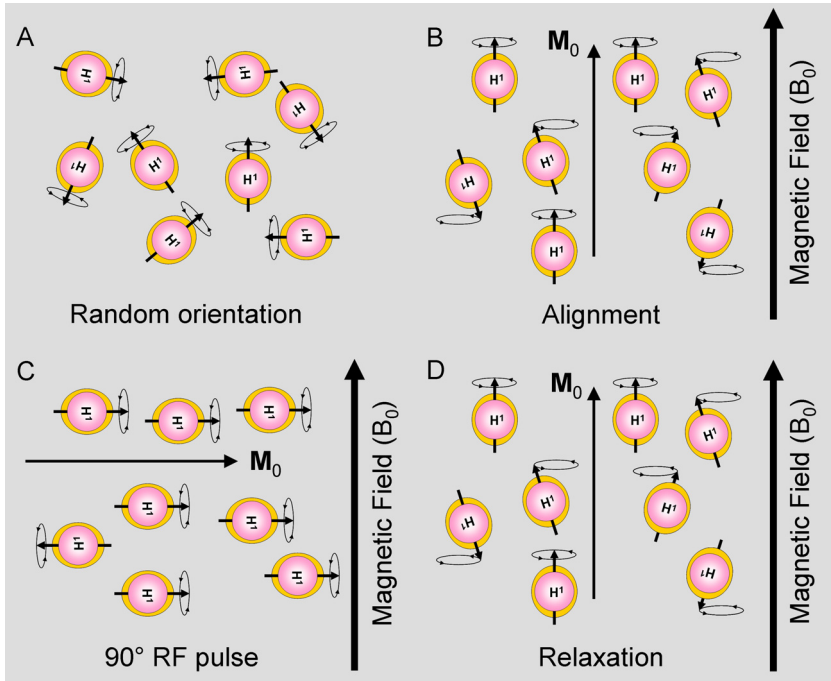


FIGURE 1.5 Basic principles of MRI. The magnetic moment of the hydrogen nuclei (^1H) has an axis and a direction (black arrow). Initially, these directions are randomly oriented (A), but when they are exposed to an external magnetic field (B_0), they precess around it. There will be a slight preference to align with the magnetic field (B). The sum of all magnetic moments forms a macroscopic net magnetization (M_0). When an RF pulse is applied (C), the net magnetization is flipped at an angle and all the ^1H protons start to precess in phase. This phase coherence is lost due to interactions (T2 relaxation). After the RF pulse is switched off, the net magnetization starts to return back to its original alignment along the applied magnetic field (T1 relaxation) (D).

The product of RF amplitude and duration determines the angle of rotation. Thus, if this RF pulse is applied for a sufficient time, it can cause the net magnetization to position at 90 degrees, 180 degrees or any other angle from the main magnetic field, which is known as the flip angle of the RF pulse.

In general, the direction of an angle can be expressed on an x-axis, y-axis and z-axis, where the z-axis is parallel to the main magnetic field. Once the RF pulse has caused the net magnetization (M_0) to make an angle with the z-axis, it can be split into two components: the longitudinal component (M_z), which is parallel to the z-axis, and the transverse component (M_{xy}) which rotates in the xy-plane (Figure 1.6). Of these, only the M_{xy} component will generate a detectable MR-signal. These two components are important to understand the relaxation of the net magnetization back to its original position along the main magnetic field after the RF pulse is switched off (Figure 1.5d).

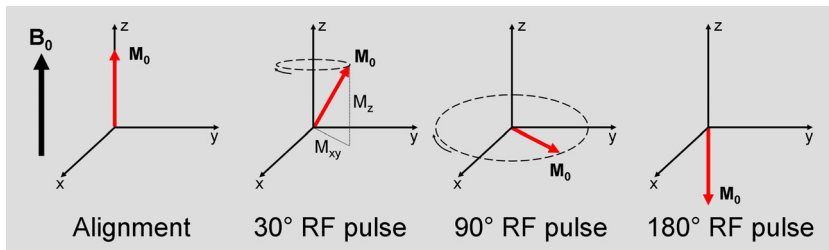


FIGURE 1.6 When an RF pulse is applied, the net magnetization (M_0) (red arrow) is flipped at an angle, which produces two magnetization components: a longitudinal component (M_z), which is parallel to the main magnetic field, and a transverse component (M_{xy}), which rotates around the main magnetic field.

T1 and T2 Relaxation

Immediately after the RF pulse, the net magnetization (M_0) starts to return back to its original state. This process is known as relaxation and it is caused by the exchange of energy to its surrounding tissue. Relaxation occurs simultaneously along the longitudinal and transverse component.

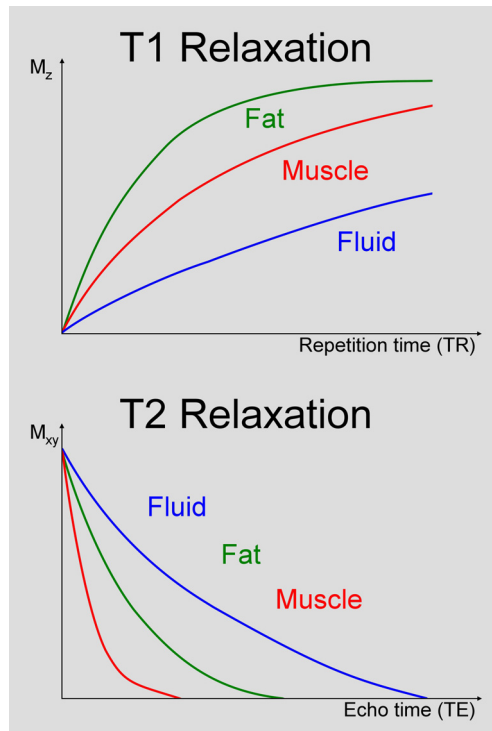


FIGURE 1.7 **T1 relaxation.** Application of a 90° RF pulse causes the longitudinal magnetization (M_z) to become zero. Over time, the longitudinal magnetization will recover. The T1 relaxation of fat is typically faster than the T1 relaxation of muscle and fluids. **T2 relaxation.** The transverse magnetization (M_{xy}) has a maximum amplitude as the spins rotate in phase due to the application of a 90° RF pulse. The amplitude decays as the spins move out of phase.

The rate with which the net magnetization regains its longitudinal component in the direction of the main magnetic field is called T1 relaxation. The longer the M_z component is allowed to re-grow before a subsequent RF pulse is applied, the more signal will be available then.

The second relaxation occurs along the transverse component. The protons that precessed in synchrony around the main magnetic field start to dephase, which is called T2 relaxation. As the precessions become more and more dephased, the magnitude of M_{xy} dwindles, and the signal detected will decrease.

Relaxation occurs in all tissues, but the values of T1 and T2 relaxation are different for each tissue. For example, compared to fat, free water is unfavorable for energy exchange at the Larmor frequency and it has therefore a longer T1 relaxation time (Figure 1.7). Furthermore, free water contains small molecules that are relatively far apart and move rapidly. It has therefore a slower T2 relaxation compared to tissue with a high macromolecular content (e.g. muscle) (Figure 1.7). Hence, based on when the image is taken after the RF pulse, different tissues are visualized with different contrast on the MR images due to their differences in relaxation time. There might even be a difference in contrast within the same tissue according to whether it is in a normal or diseased state.

Spin-echo sequences

One way to recover from the T2 relaxation that occurs when the RF pulse ends, is to apply a spin-echo sequence (Figure 1.8). After the 90° RF excitation pulse, protons that were in phase begin to dephase in the transverse plane. After a certain amount of time, a 180° RF pulse can be applied causing the spins to rotate in the opposite direction. As a result, rather than to continue dephasing, the spins will begin to align again, and at a certain time point, a new signal maximum is reached. This is then once again followed by dephasing. The increased signal caused by rephasing is called a spin echo. The time between the first 90° RF pulse and the peak of this echo is called the echo time (TE). Furthermore, in a sequence of RF pulses, the repetition time (TR) is the time lapsing between two RF excitation pulses, which would be the time between two consecutive 90° RF pulses when applying a spin-echo sequence (Figure 1.8).

As described above, one of the most important advantages of MR imaging is the ability to generate contrast between different soft tissue types. This is because different types of soft tissue have different characteristic T1 and T2 relaxation times. The MR signal generated for a particular tissue depends on its relaxation properties, and the contrast between tissues is controlled by the choice of sequence parameters. The spin-echo sequence can produce T1-weighting where fluid appears dark on the MRI images. In order to generate a T1-

Spin-Echo Sequence

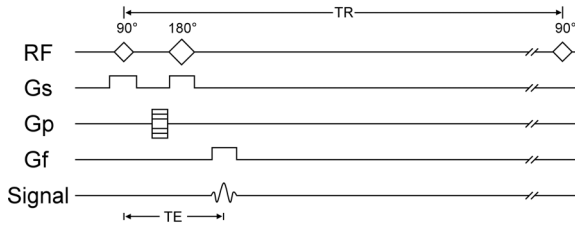


FIGURE 1.8 A spin-echo pulse sequence diagram showing the relative timing of the RF and gradient pulses to localize and encode the MR signal for image formation. The initial 90° RF pulse is followed by a 180° RF pulse to refocus the spins. Gs, Gp and Gf are the slice selective, phase encoding and frequency encoding gradients, respectively. Signal represents the signal received from the slice of interest in the body. TR = repetition time; TE = echo time.

Turbo Spin-Echo Sequence

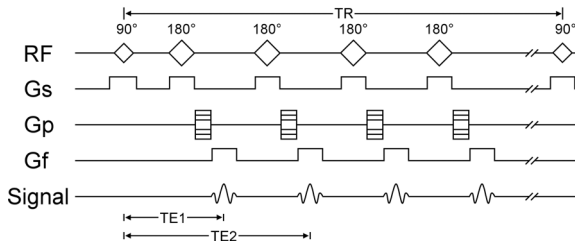


FIGURE 1.9 A turbo spin-echo pulse sequence diagram showing the relative timing of the RF and gradient pulses to localize and encode the MR signal for image formation. The initial 90° RF pulse is followed by multiple 180° RF pulse to refocus the spins several times. Gs, Gp and Gf are the slice selective, phase encoding and frequency encoding gradients, respectively. Signal represents the signal received from the slice of interest in the body. Multiple echoes are created during one repetition time (TR), which greatly reduces the acquisition time. TE = echo time.

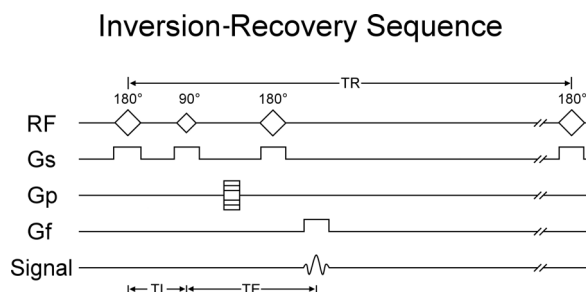


FIGURE 1.10 An inversion-recovery spin-echo pulse sequence diagram showing an initial 180° RF pulse, applied to invert the magnetization, followed by a 90° RF excitation pulse at a pre-determined inversion time (TI) to null the fat signal while maintaining water and soft tissue signal. Abbreviations as in Figure 1.9.

weighted image, both the repetition time and echo time have to be short. A spin-echo sequence can also produce T2-weighting, where water appears bright on the MRI images. Thus, T2-weighting is of specific interest for this thesis since it enables visualization and possibly quantification of edema in the myocardium. In order to generate a T2-weighted image, both the repetition time and echo time have to be long.

The spin-echo sequence is a commonly used pulse sequence. However, it may take an extensive amount of time to acquire all the data using a conventional spin-echo sequence. This problem has been addressed by applying a turbo spin-echo sequence (Figure 1.9). In addition to a regular spin-echo sequence, multiple 180° RF pulses are used to create multiple echoes. Hence, more data is acquired during one repetition time period, which greatly reduces the total image acquisition time. An issue with turbo spin-echo sequences is their many high energy RF pulses. In order to stay within safety limits to prevent patient heating, turbo spin-echo sequences can be difficult to apply at higher field strengths without compromising image quality.

Inversion-recovery sequences

The inversion-recovery sequences are used to give T1-weighting. However, they can also be used for suppressing unwanted signals in MR images, while T1- and

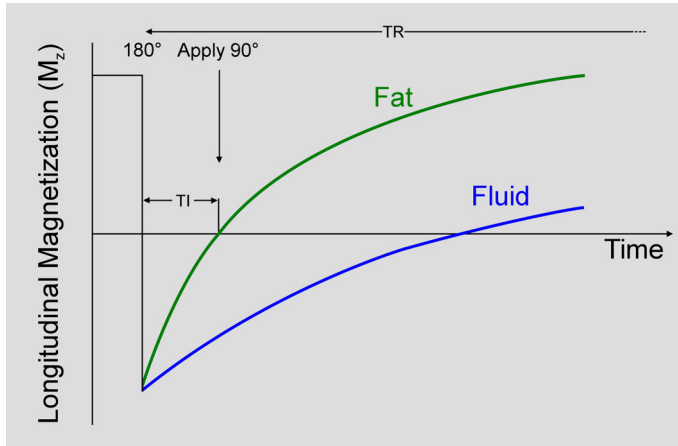


FIGURE 1.11 T1 relaxation of fat and fluid (water) after a 180° RF pulse in an inversion-recovery pulse sequence. When the 90° RF pulse flips the net magnetization into the transverse plane at TI (inversion time), the magnetization of fat is zero and will not provide any signal on the MRI image. TR = repetition time.

T2-weighting can still be controlled through selection of TR and TE. In T2-weighted images, both fat and edema typically appear bright, which could potentially affect accurate assessment of the size of the myocardium at risk. Thus, it would be favorable to suppress the signal acquired from fat.

The difference between an inversion-recovery sequence and a spin-echo sequence is the occurrence of one or more 180° RF pulses prior to the regular spin-echo sequence (Figure 1.10). The 180° RF pulse causes an initial inversion of the longitudinal magnetization (M_z), as shown in Figure 1.11. As soon as the RF pulse is switched off, T1 relaxation occurs in all tissues at different rates, as described earlier. When the M_z from the tissue to be suppressed (fat) crosses the transversal plane, application of a 90° RF pulse will rotate all M_z into the transverse plane. Since the signal from fat is zero, there is nothing to rotate into the transverse plane. Hence, this tissue will be dark on the MRI image. The time between the initial 180° RF pulse and the start of the spin-echo sequence is called inversion time (TI). Fat has a relatively fast T1-relaxation, which indicates that the inversion time is rather short. This sequence is therefore often called short TI inversion recovery (STIR).

Other imaging sequences

Steady state free precession (SSFP) cine imaging requires very short repetition times, on the order of 4 ms. This makes it suitable for data acquisition throughout the cardiac cycle with good temporal resolution. As balanced SSFP sequences also have excellent contrast between blood and myocardium, they are the sequence of choice for imaging of myocardial function. Such short repetition times can only be achieved by using a gradient-echo sequence. Compared to the spin-echo sequences, gradient-echo sequences only have one RF pulse within each TR interval. As opposed to 90° or 180°, the flip angle of the RF pulse in gradient-echo sequences commonly varies between 10° and 80° degrees. This allows the net magnetization (M_0) to remain closer to its equilibrium along the main magnetic field, which results in a larger signal compared to multiple 90° RF pulses with short repetition times. The contrast generated in SSFP images is dependent on the ratio between T2-weighting and T1-weighting. Larger flip angles provide more T1-weighting, whereas smaller flip angles provide more T2-weighting to the images. Thus, these sequences can potentially be used to visualize edema within the myocardium.

Despite the excellent contrast that can be generated by MRI without administration of a contrast agent, some situations may benefit from increased tissue contrast obtained by the presence of a paramagnetic contrast agent. In these situations, a gadolinium-based contrast agent can be administered intravenously, which will distribute freely into the extracellular space. The concentration of gadolinium in the myocardium is directly proportional to the relative amount of extracellular space. In the situation of acute myocardial infarction, the extracellular space in the infarcted region is increased due to the presence of edema and the rupture of cell membranes. Thus, this myocardium contains more gadolinium compared to viable myocardium. Gadolinium has paramagnetic properties that affect the T1 relaxation time of tissues.⁶⁹ Therefore, T1 relaxation will be shorter in tissue containing more gadolinium compared to tissue with less gadolinium. In order to visualize the differences in T1 relaxation, the above mentioned inversion-recovery sequence can be applied, now with a longer inversion time (TI), adjusted to null the signal from viable myocardium. This way, myocardium that contains more gadolinium is hyper-enhanced whereas viable myocardium will appear black.

Imaging planes

MRI has the possibility to acquire images in any plane. This is done by utilizing the three gradient coils to define and encode any oblique plane. The imaging

projections in three different views: the 2 chamber view, 3 chamber view and the 4 chamber view (Figure 1.12).

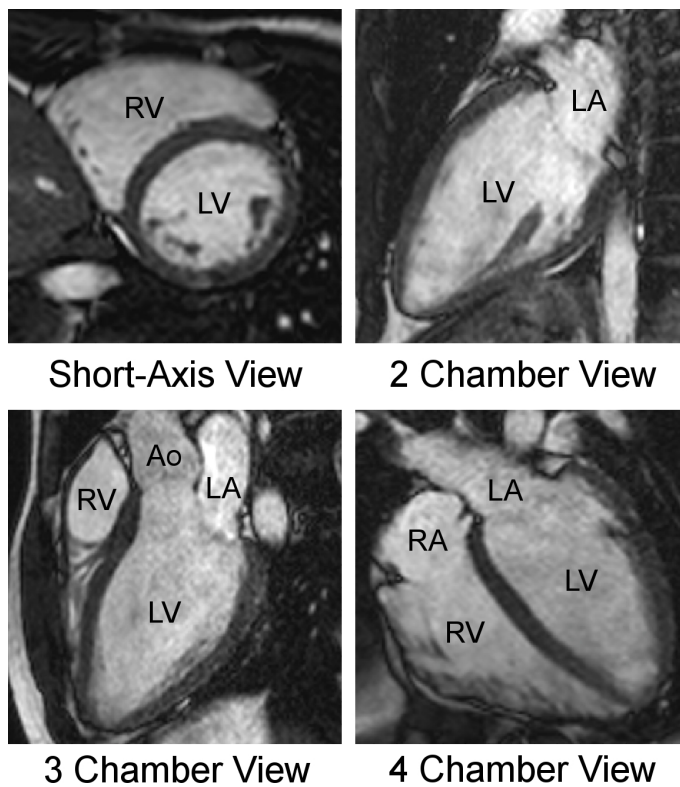


FIGURE 1.12 Example of short- and long-axis views of the heart. RV = right ventricle; LV = left ventricle; LA = left atrium; RA = right atrium; Ao = aorta.

Chapter 2

Aims of the Work

The general aim of this thesis was to explore the use of CMR imaging to quantitatively and qualitatively assess the myocardium at risk after acute coronary occlusion.

The specific aims for each studie were:

- I. To validate the measurements of the myocardium at risk on T2-weighted imaging over time, in comparison with myocardial perfusion SPECT in humans with acute myocardial infarction, and to assess the amount of salvaged myocardium after 1 week.
- II. To assess the ability of endocardial extent of infarction assessed by late gadolinium enhanced CMR to predict myocardium at risk as compared to T2-weighted imaging in patients with first-time early reperfused myocardial infarction.
- III. To explore the relationship between early gadolinium enhancement and T2-weighted imaging with regards to myocardium at risk in patients with first-time reperfused acute myocardial infarction.
- IV. To test the ability of *ex vivo* T2-weighted imaging to assess MaR compared to myocardial perfusion SPECT and to investigate whether MaR could also be assessed by *ex vivo* T2-weighted imaging after injection of a gadolinium-based contrast agent in pigs with experimentally induced myocardial infarction.

Chapter 3

Materials and Methods

All protocols and procedures were approved by the regional research ethics committee at Lund University, Sweden. All patients (Study I, II and III) were recruited at the Skåne University Hospital and gave their written informed consent to participate in the studies.

3.1 Human studies (Study I, II and III)

3.1.1 Study population and design

Patients presenting with acute ST-elevation myocardial infarction (STEMI) due to a single occluded coronary artery, as seen by angiography, were included in the studies. Patients with a non-occluded coronary artery, contraindications for CMR such as metal implants, claustrophobia or signs of an old infarction were excluded. All patients were treated by primary PCI with coronary stenting and a GPIIb/III inhibitor, resulting in Thrombolysis in Myocardial Infarction (TIMI) grade 3 flow in the culprit artery. All patients were transferred to the coronary care unit for conventional therapy that included a thrombocyte aggregation inhibitor, ACE inhibitor, beta receptor inhibitor, and a statin. All included patients had an uncomplicated time course between the acute phase and follow-up.

Study I

Before primary PCI, ^{99m}Tc -tetrofosmin was administered intravenously, and myocardial perfusion SPECT imaging was performed approximately 3 to 4 hours after primary PCI to determine the MaR. For comparison, CMR with

T2-weighted imaging was performed 1 week after primary PCI. In 1 patient, no adequate T2-weighted images could be obtained at 1 week for determination of MaR. To determine the evolution of the increase in T2-weighted signal, early imaging was performed within 1 day in 8 patients and within 2 days in 2 patients (hereafter described as day 1), and 9 patients underwent CMR follow-up at 6 weeks and 6 months. In addition to T2-weighted imaging, all patients underwent late gadolinium enhanced (LGE) CMR with administration of gadolinium at 1 week for determination of the final infarct size.

Study II

CMR with T2-weighted imaging was performed within the first week after primary PCI in all patients to determine the MaR. For comparison, all patients underwent LGE CMR during the same examination with administration of gadolinium to determine both the MaR by endocardial extent of infarction as well as the final infarct size.

Study III

CMR with T2-weighted imaging was performed within the first week after primary PCI to determine MaR. For comparison, steady state free precession (SSFP) cine imaging was performed approximately 8 minutes after administration of gadolinium for determination of MaR. In addition, LGE CMR was performed to determine final infarct size. For 1 patient, myocardial infarct size could not be determined due to poor LGE image quality resulting from frequent arrhythmias. Another patient had a clinical history of prior infarction in a coronary artery territory different from that supplied by the current occluded vessel. This patient had, however, no sign of infarction by LGE imaging in the part of the myocardium previously reported to be infarcted, and was therefore included in the study.

3.1.2 Myocardial perfusion SPECT

Imaging

Patients were injected with 500 to 700 MBq ^{99m}Tc -tetrofosmin (Amersham Health, Buckinghamshire, United Kingdom), depending on body weight. Myocardial perfusion SPECT was performed according to the standard clinical protocol, using a dual-head camera. Patients were imaged with either an ADAC

Vertex camera (ADAC, Milpitas, CA, USA) or a cardiac dedicated GE Ventri camera (GE Healthcare, Buckinghamshire, United Kingdom). The patients were placed in a supine position and imaged in steps of 5.6° using a 64×64 matrix with a pixel size of 5.02 mm for the Philips SKYLight camera and a pixel size of 6.4 mm for the GE Ventri camera. Image acquisition time was approximately 15 minutes, which was extended to 25 minutes when imaging was performed after 3 hours.

Short-axis images covering the left ventricle were reconstructed using a commercial application (AutoSpect+InStill™ 6.0, ADAC, Milpitas, CA, USA). Iterative reconstruction using maximum likelihood-expectation maximization (MLEM) was performed with a low-resolution Butterworth filter with a cut-off frequency set to 0.6 of Nyquist and order 5.0. No attenuation or scatter correction was applied.

Image analysis

The endocardial and epicardial borders of the left ventricle (LV) as well as the MaR were determined using an in-house developed segmentation software Segment v1.7 (<http://segment.heiberg.se>).^{65, 70} The algorithm for segmenting the LV finds the centerline through the LV wall and identifies the endocardium and epicardium based on individually estimated wall thickness and signal intensities. In few patients, manual adjustment of the automatic delineation was required in the LV outflow region. The perfusion defect was determined by an automated algorithm that considers myocardium with less than 55% of maximal LV counts as being ischemic.

3.1.3 Cardiac magnetic resonance

Imaging

CMR was performed on either of two 1.5T systems: Siemens, Magnetom Vision (Siemens, Erlangen, Germany) with a CP body array coil, or Philips Intera CV/Achieva (Philips, Best, the Netherlands) with a cardiac synergy coil. All subjects were placed in supine position and images were acquired at end-expiratory breath hold with electrocardiographic gating. After initial scout images to locate the heart, SSFP cine imaging, T2-weighted imaging, and LGE imaging was performed in all patients.

Short- and long-axis, retrospectively gated SSFP cine images, covering the left ventricle from base to apex were acquired before (Study I, II, and III) and

approximately 8 minutes after administration of 0.2 mmol/kg extracellular gadolinium-based contrast agent (gadoteric acid, Gd-DOTA; Guerbet, Gothia Medical AB, Billdal, Sweden) (Study III). These images were referred to as early gadolinium enhancement (EGE) images. Typical image parameters were: echo time, 1.4 ms; repetition time, 2.9 ms; flip angle, 60 degrees; image resolution, 1.5 x 1.5 x 8 mm; slice gap, 0 mm.

In Study I and II, a T2-weighted triple inversion turbo spin-echo sequence (T2-STIR) was employed to depict MaR. T2-weighted images were acquired in the short-axis view, covering the LV from the base to apex. Image parameters for T2-weighted imaging were: echo time, 43 ms (Siemens), or 100 ms (Philips); repetition time, 2 heart beats; number of averages, 2; inversion time, 180 ms; image resolution, 1.5 x 1.5 mm; slice thickness, 10 mm (Siemens), or 8 mm with a slice gap of 2 mm (Philips). In Study III, similar image parameters were used as for those patients imaged with the Philips system in Study I and II, with the difference that an image resolution of 1.5 x 1.5 x 8 mm was used with a 0 mm slice gap.

Approximately 15-30 minutes after intravenous administration of gadolinium, long- and short-axis LGE images were acquired covering the left ventricle from base to apex. The LGE images were acquired with an inversion-recovery sequence with the following imaging parameters: slice thickness, 10 mm; field of view, 380 mm; matrix, 126 x 256; flip angle, 25 degrees; repetition time, 100 ms; echo time, 4.8 ms (Siemens) or slice thickness, 8 mm; field of view, 340 mm; flip angle, 15 degrees; repetition time, 3.14 ms; echo time, 1.58 ms (Philips). Inversion time was adjusted to null the signal from viable myocardium.

Image analysis

All CMR images were analyzed using an in-house developed segmentation software Segment v1.7 or above (<http://segment.heiberg.se>).^{71, 72}

To assess the MaR by T2-weighted imaging, endocardial and epicardial borders of the left ventricle were traced manually in all short-axis slices. An incomplete dark-blood preparation sometimes leaves a bright rim blood artifact adjacent to the endocardium. This so-called slow flow artifact can affect delineations when differentiating endocardium from blood pool. Therefore, SSFP cine images were used for side-by-side comparison with the T2-weighted images in the same cardiac phase, to verify wall thickness. The papillary muscles were excluded from the myocardium. The hyperintense regions within the myocardial borders were then delineated manually in all short-axis slices by independent observers blinded to any other data. The MaR was defined as the

total amount of hyperintense myocardium in all short-axis slices and expressed as percentage of LV myocardium. If present, an area of hypointense signal within the area of increased signal intensity was included in the MaR. Furthermore, in Study III, the contrast ratio for the T2-weighted images was determined for each patient as the mean intensity in the MaR divided by the mean intensity in remote myocardium.

To derive the MaR from the EGE images 8 minutes after injection of gadolinium, endocardial and epicardial borders of the left ventricle were traced in all short-axis slices in end-diastole and end-systole. This was then followed by manual delineation of the hyperintense regions in both end-diastole and end-systole, by two observers blinded to both the T2-weighted and LGE images. The values of MaR in end-diastole and end-systole were averaged and expressed as percentage of the LV. The contrast ratio for the EGE images was determined for each patient as the mean intensity in the MaR divided by the mean intensity in remote myocardium.

The infarcted myocardium was automatically quantified from the short-axis LGE images, after manual tracing of the endocardial and epicardial borders of the LV, according to a previous described method.⁷² Papillary muscles were excluded from analysis. The LGE myocardium was then defined using a computer algorithm that takes into consideration partial volume effects within the infarcted region. Manual adjustments were made when the computer algorithm was obviously wrong. If present, a hypointense signal within the area of LGE (microvascular obstruction) was included in the analysis as being completely infarcted. Finally, myocardial infarct size was expressed as percentage of the LV.

The MaR by endocardial extent of infarction (Study II) was determined in each short-axis slice by measuring the circumferential distance between the lateral borders of the LGE region (Figure 3.1). The lateral borders of LGE were used since the mid-mural LGE might extend beyond the endocardial circumferential edges. The endocardial extent of infarction was then defined as the sum of the LGE endocardial circumferential distance in each short-axis slice, divided by the total endocardial extent of the LV (Figure 3.1).

Myocardial salvage was defined as $100 * ([\text{MaR} - \text{infarct size}] / \text{MaR})$.

3.1.4 Statistical analysis

The software SPSS version 17.0 or above was used for all statistical analysis. Data is presented as mean \pm standard deviation (SD) unless otherwise is specified. A value of p below 0.05 was considered statistically significant. Pearson's correlation was used to determine the relationship between MaR

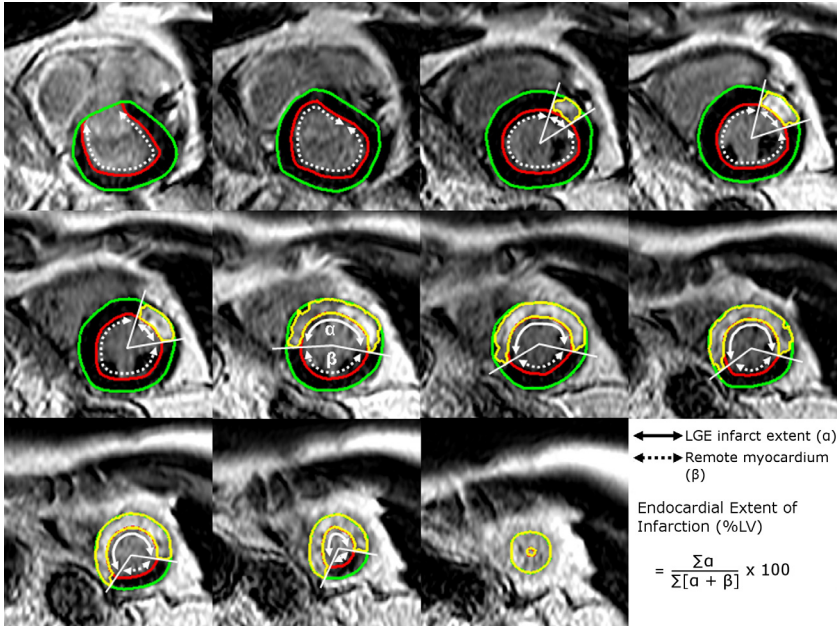


FIGURE 3.1 Late gadolinium enhanced (LGE) CMR showing short-axis slices covering base (top left) to apex (bottom right) in a patient with an occlusion of the left anterior descending coronary artery. The endocardial borders are traced in red and the epicardial borders are traced in green. The infarct is shown as an LGE area within the myocardial borders and is delineated in yellow. The circumferential endocardial extent of LGE is marked by the solid arrow (α) and the remote myocardium is marked by the dashed arrow (β). The endocardial extent of MI was defined as the sum of the LGE circumferential endocardial extent in each short-axis slice ($\sum \alpha$), divided by the total endocardial extent ($\sum [\alpha + \beta]$) of the LV. In this patient, the MaR by T2-weighted imaging and LGE endocardial extent was 37% and 32%, respectively. The corresponding infarct size was 32%, resulting in a myocardial salvage of 13% and 0% when measured with T2-weighted imaging and LGE endocardial extent, respectively.

assessed by T2-weighted imaging and the MaR determined by myocardial perfusion SPECT (Study I), endocardial extent of infarction (Study II) and early gadolinium enhancement (Study III).

In Study I, a paired t-test was used to detect differences in MaR between T2-weighted imaging and myocardial perfusion SPECT, differences in MaR by T2-weighted imaging at different time points, and differences between MaR by T2-weighted imaging and final infarct size by LGE imaging. The agreement between T2-weighted imaging and myocardial perfusion SPECT was expressed as mean difference \pm SD, and the limits of agreement were shown in a Bland-Altman graph as mean difference \pm 2 SD.

In Study II, the agreement between T2-weighted imaging and endocardial extent of infarction was expressed as mean difference \pm SD, and the limits of agreement were shown in a Bland-Altman graph as mean \pm 2 SD. The difference between using T2-weighted imaging and endocardial extent of infarction for determination of MaR to derive myocardial salvage was assessed by a paired t-test.

In Study III, the agreement between T2-weighted imaging and EGE was expressed as mean difference \pm SD, and the limits of agreement were shown in a Bland-Altman graph as mean \pm 2 SD. The interobserver variability was expressed as mean difference \pm SD. A paired t-test was used to compare the means of the contrast ratio between MaR and remote myocardium for both T2-weighted imaging and EGE. Pearson's correlation was used to determine the relationship between T2-weighted imaging and EGE with regards to determination of myocardial salvage.

3.2 Animal studies (Study IV)

3.2.1 Experimental preparation

Healthy domestic male and female juvenile pigs weighing 42-53 kg were anesthetized with 12.5 mg/kg thiopental (Pentothal, Abbott, Stockholm, Sweden) followed by intubation with cuffed endotracheal tubes. Mechanical ventilation with a mixture of nitrous oxide (70%) and oxygen (30%) was established in a volume-controlled mode, adjusted in order to obtain normocapnia (pCO₂: 5.0-6.0 kPa). A slow infusion of 1 µg/ml fentanyl (Fentanyl, Pharmalink AB, Stockholm, Sweden) in buffered glucose (25 mg/ml) was started at a rate of 2 ml/min and adjusted if needed. During balanced anesthesia, thiopental was titrated towards animal requirements with small bolus doses. The pigs were continuously monitored by electrocardiography. Heparin (200 IU/kg) was given intravenously at the start of the catheterization. A 6 F introducer

sheath (Boston Scientific Scimed, Maple Grove, MN, USA) was inserted into the surgically exposed left carotid artery upon which a 6 F FL4 Wiseguide™ (Boston Scientific Scimed, Maple Grove, MN, USA) was inserted into the left main coronary artery. The catheter was used to place a 0.014-inch PT Choice™ guide wire (Boston Scientific Scimed, Maple Grove, MN, USA) into the distal portion of the left anterior descending coronary artery (LAD). A 3.0-3.5 × 15 mm Maverick monorail™ angioplasty balloon (Boston Scientific Scimed, Maple Grove, MN, USA) was then positioned distal to the first diagonal branch of the LAD.

3.2.2 Experimental protocol

An overview of the experimental protocol is shown in Figure 3.2.

In 18 domestic pigs, a percutaneous coronary intervention balloon was inflated in the left anterior descending artery for either 30 or 40 minutes. Two different ischemia times were chosen to vary the amount of infarction within the MaR. An angiogram was performed after inflation of the balloon and before deflation of the balloon in order to verify total occlusion of the coronary vessel and correct balloon positioning. Ten to twenty minutes prior to deflation, the animal was intravenously injected with 1000 MBq ^{99m}Tc-tetrofosmin (Amersham Health, Buckinghamshire, United Kingdom). After deflation of the balloon, a subsequent angiogram was performed to verify restoration of blood flow in the previously occluded artery, which was then followed by a 4 hour reperfusion period. Fifteen minutes before sacrificing the pigs, 60% (11/18) of the pigs were injected intravenously with a 0.2 mmol/kg gadolinium-based contrast agent (gadopentate dimeglumine, Magnevist, Bayer Pharma, Berlin, Germany). All pigs were sacrificed by injection of a saturated potassium chloride solution, followed by explantation of the hearts. After explantation, the atria were removed and the left and right ventricles were rinsed and filled with balloons containing deuterated water. The hearts were then suspended in air hanging in a cylindrical plastic container (diameter 13 cm, height 12 cm) and imaged by myocardial perfusion SPECT and CMR imaging for determination of MaR. Following imaging, the hearts were cut into 5 mm thick short-axis slices that were immersed in a 1% triphenyltetrazolium chloride (TTC) solution (Sigma-Aldrich, Stockholm, Sweden) in saline at 34 degrees Celsius for approximately 5-7 minutes. The TTC-stained short-axis slices were then photographed under blue light to verify infarction. The hearts from 3 pigs were placed

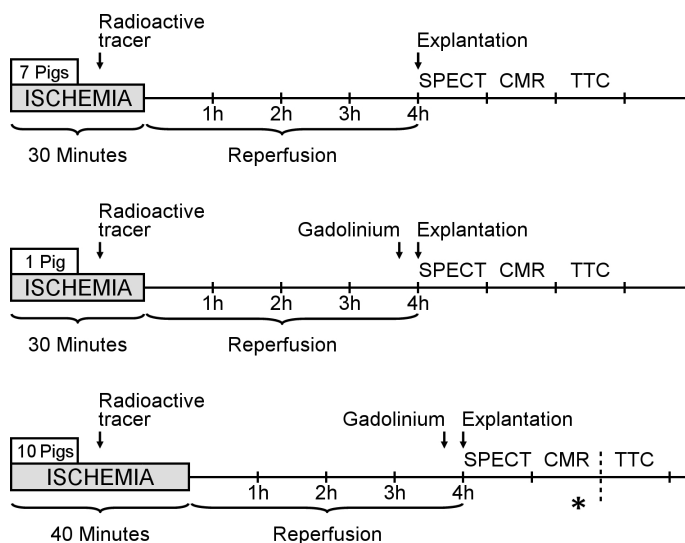


FIGURE 3.2 A schematic overview of the experimental study protocol from balloon inflation to TTC-staining. Ischemia duration was varied (30 and 40 min.) to vary the amount of infarction within the myocardium at risk. (*) After the first CMR imaging, 3 pig hearts were stored at 4 degrees Celsius for approximately 24 hours after which they underwent a second CMR imaging session and TTC-staining. CMR = cardiac magnetic Resonance. SPECT = single-photon emission computed tomography. TTC = triphenyltetrazolium chloride.

in a refrigerator at 4 degrees Celsius for approximately 24 hours, followed by a second CMR imaging session, before TTC-staining was performed.

3.2.3 Myocardial perfusion SPECT

Imaging

The excised *ex vivo* heart underwent myocardial perfusion SPECT imaging with a dual head camera (Philips SKYLIGHT, Best, the Netherlands) and a vertex high

resolution collimator (ADAC Vertex, Milpitas, CA, USA) at 32 projections (40 s per projection) with a 64×64 matrix, yielding a digital resolution of $4.24 \times 4.24 \times 4.24$ mm. Image acquisition time was approximately 30 minutes.

Iterative reconstruction using MLEM was performed with a low-resolution Butterworth filter with a cut-off frequency set to 0.6 of Nyquist and order 5.0. No attenuation or scatter correction was applied. Finally, a short-axis image stack was reconstructed (AutoSPECT Plus, Pegasys software version 5.01, Philips, Best, the Netherlands).

Image analysis

To ensure co-registration of endocardial and epicardial borders of the myocardium, an image fusion module was implemented into the software segment for registration of the endocardial and epicardial borders defined in the CMR images to be transferred to the myocardial perfusion SPECT images (Figure 3.3). The fusion module allows for co-registration by rigid body motion (translation and rotation). Fusion of the myocardial perfusion SPECT and CMR images was then performed by overlaying the myocardial perfusion SPECT images, with variable translucency, on top of the delineated CMR images. The combined fusion image was used to visually ensure optimal co-registration in all three orthogonal imaging planes. If necessary, manual adjustments were made.

The perfusion defect was determined by an automated algorithm that considers myocardium with less than 55% of maximal LV counts as being ischemic.⁷⁰ In some pigs minor adjustments were made in the most basal short-axis slice containing a perfusion defect within the delineated left ventricle not depicted by the computer algorithm.

3.2.4 Cardiac magnetic resonance

Imaging

CMR imaging on the *ex vivo* hearts was performed using a 1.5T Philips Achieva (Philips, Best, the Netherlands) with a quadrature head coil. Initial scout images were acquired to locate the heart. All hearts were imaged with a T2-weighted double inversion black blood breath hold sequence (T2-TSE) with an asymmetric turbo spin-echo, modified to enhance differences in signal between water and normal myocardium. T2-TSE images were acquired in the short- and long-axis views, covering the left ventricle from base to apex with a simulated

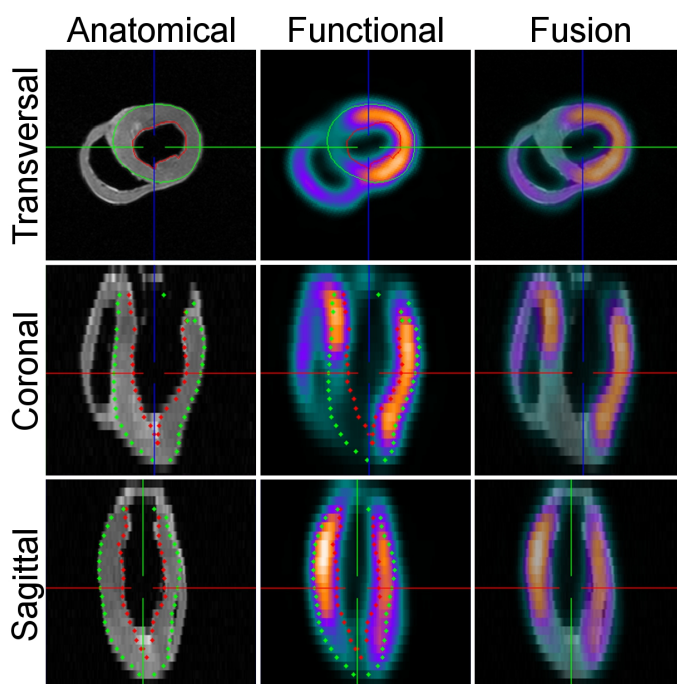


FIGURE 3.3 Co-registration of T2-weighted CMR (left column) with myocardial perfusion SPECT (middle column) and fusion of the two image modalities (right column) in three different orthogonal imaging planes. The left ventricular endocardial border (red dots) and epicardial border (green dots) from the T2-weighted CMR images are copied to the myocardial perfusion SPECT images.

heart rate at 60 beats per minute. Imaging parameters for the T2-TSE sequence were: field-of-view, 140 mm; echo time, 60 ms; repetition time, 2 heart beats; number of averages, 2; black blood inversion delay, 574 ms; acquisition matrix size, 140 x 124; image resolution, 1.0 x 1.13 mm; slice thickness, 4 mm; slice gap, 0 mm; no parallel imaging.

For demonstration of the effect of gadolinium on a standard clinical T2-weighted triple inversion turbo spin-echo sequence (T2-STIR), two hearts were also imaged with such a clinical T2-weighted sequence, covering the LV from base to apex. One heart was imaged without the presence of gadolinium and one heart was imaged with the presence of gadolinium. Imaging parameters for the T2-STIR sequence were: simulated heart rate at 60 beats per minute. Imaging parameters for the T2-STIR sequence were: field-of-view, 140 mm; echo time, 117 ms; repetition time, 2 heart beats; number of averages, 2; black blood inversion delay, 879 ms; acquisition matrix size, 280 x 281; image resolution, 0.5 x 0.5 mm; slice thickness, 5 mm; slice gap, 0 mm; no parallel imaging.

Image analysis

The endocardial and epicardial borders of the LV were traced manually with inclusion of the papillary muscles. In all short-axis slices, the hyperintense regions were delineated manually by independent observers blinded to the myocardial perfusion SPECT data. If present, an area of hypointense signal within the area of increased signal intensity, either due to microvascular obstruction or presence of gadolinium, was included in the MaR. The MaR was then defined as the total amount of hyperintense myocardium in all short-axis slices and expressed as percentage of LV myocardium.

3.2.5 Statistical Analysis

SPSS version 18.0 (Chicago, Illinois, USA) was used for statistical analysis. Continuous variables are presented as mean \pm SD and a value of p below 0.05 was considered statistical significant. The Spearman's rank correlation was used to determine the relationship between MaR assessed by T2-weighted imaging and myocardial perfusion SPECT. The interobserver variability was expressed as mean difference \pm SD. The agreement between T2-weighted imaging and myocardial perfusion SPECT was expressed as mean difference \pm SD, and the limits of agreement were expressed as mean \pm 2 SD. A Wilcoxon Signed Rank test was performed to determine the bias between the two difference methods for assessment of MaR.

Chapter 4

Results and Comments

4.1 Validation of T2-weighted imaging (Study I)

Earlier studies have demonstrated the use of T2-weighted imaging during acute coronary occlusion, in both reperfused and non-reperfused infarcts, and validated T2-weighted imaging for MaR in animals.⁷³⁻⁷⁷ There were, however, no validation studies in humans for the quantification of MaR using T2-weighted imaging. Hence, the purpose of Study I was to validate T2-weighted imaging to determine MaR in comparison with myocardial perfusion SPECT in humans with first-time acute coronary occlusion.

In agreement with studies on humans^{75, 78} and animals,^{74, 76} the area with high T2 signal exceeded the area of irreversible injury seen by LGE imaging (Figure 4.1). The amount of edema present after 1 week was similar to the amount of edema at 1 day after reperfusion ($31 \pm 6\%$ and $29 \pm 7\%$ of LV, respectively), and there was no significant difference between these two measurements and the MaR assessed by myocardial perfusion SPECT ($p = 0.16$ and $p = 0.49$, respectively). Furthermore, the amount of edema present after 1 week correlated strongly with the MaR assessed by myocardial perfusion SPECT ($r^2 = 0.70$, $p < 0.001$) (Figure 4.2). Hence, T2-weighted imaging can be used to assess the MaR up to one week after opening of the occluded artery.

Myocardial ischemia increases cellular and extracellular osmolarity, alters plasma membrane permeability, causes cell swelling and interstitial edema.⁷⁹⁻⁸¹ Quantification of interstitial edema has been demonstrated in experimental studies of MaR after reperfusion by light microscopy, autoradiography, and contrast-enhanced inversion-recovery echo-planar CMR.^{82, 83} During reperfusion of the culprit artery, normo-osmotic blood will flow into the hyperosmotic myocardium, which creates an osmotic gradient causing water to shift towards

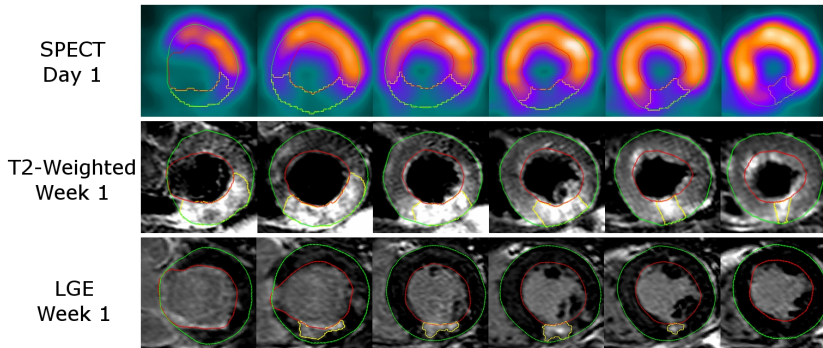


FIGURE 4.1 Short-axis slices at the same ventricular level of myocardial perfusion SPECT at day 1, T2-weighted imaging at week 1, and late gadolinium enhancement (LGE) at week 1, in a patient with reperfused right coronary artery occlusion resulting in an inferior infarct. The epicardium is traced in green, the endocardium is traced in red, and the affected region is traced in yellow. Note the similarity in size of the affected region between perfusion defect size by SPECT and T2-weighted imaging, showing that T2-weighted imaging can be used to quantify MaR up to one week after opening of the occluded vessel.

the interstitial space.⁸⁴ Thus, reperfusion further enhances the amount of edema present in the myocardium. Myocardial edema is therefore a consistent feature of acute ischemia, which can be used to assess the MaR. Furthermore, the ischemic episode causes post-ischemic stunning,³⁸ associated with a decreased contractility in the previously ischemic myocardium. This decreased contractility is likely associated with a decreased lymphatic drainage from this part of the myocardium, which may also contribute to residual increased water content seen several days after the acute event. Pathology studies in humans have shown complete resorption of this residual edema within 5 weeks after the acute coronary occlusion.⁷⁹ More recently, Aletras *et al.*⁷⁴ showed that edema was still present at the 2-month follow-up CMR in a canine model. The results of Study I showed that the size of MaR declined over time, and no evidence of edema was seen on the T2-weighted images 6 months after the acute coronary occlusion in most of the patients (Figure 4.3 and Figure 4.4). Subsequently, one may hypothesize that those patients with presence of edema at 6 months may have had residual or recurring ischemia within the same myocardial region.

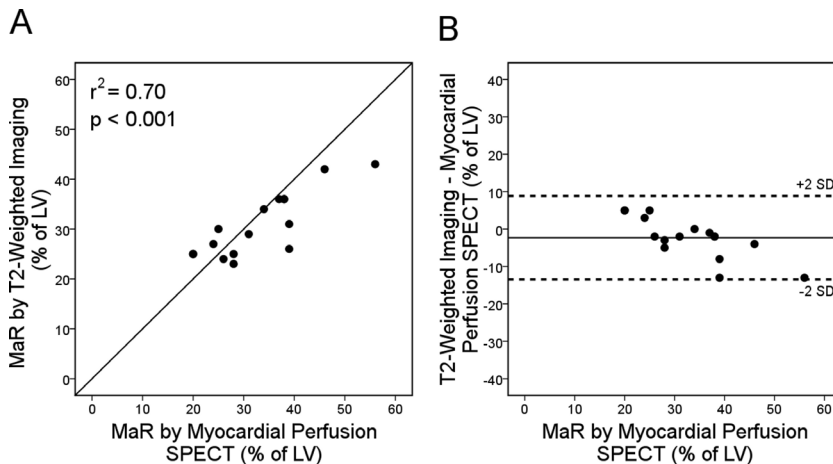


FIGURE 4.2 **A)** Relationship between T2-weighted imaging at week 1 versus myocardial perfusion SPECT for myocardium at risk. Solid line = line of identity. **B)** The limits of agreement between the two measures of MaR. The difference between the two methods was $-2.3 \pm 5.7\%$. Solid line = mean difference; dashed lines = ± 2 SD.

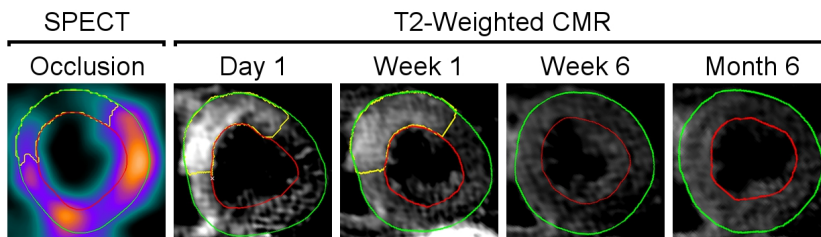


FIGURE 4.3 Mid-ventricular short-axis slices of myocardial perfusion SPECT and T2-weighted imaging over time, in a single patient with a left anterior descending coronary artery occlusion. The epicardium is traced in green, the endocardium is traced in red, and the affected region is traced in yellow. Note that the signal of the affected region on T2-weighted imaging is similar at day 1 and week 1, but disappears at week 6.

The clinical usefulness of the present study is mainly that both the MaR and final infarct size can be assessed in a single CMR imaging session 1 week after the acute coronary occlusion, without interfering with patient care in the acute setting. The relation between MaR and final infarct size enables determination of the amount of myocardial salvage, which can be used to evaluate new drugs and therapeutic procedures aimed at reducing infarct size.^{85, 86} Indeed, Ibanez *et al.*⁸⁷ recently showed that pigs treated with a beta receptor inhibitor during ongoing myocardial infarction had a 5-fold-larger myocardial salvage compared to pigs treated with a placebo. In this study, the MaR and final infarct size were assessed with T2-weighted imaging and LGE imaging. The results of Study I, in patients with primary PCI, showed that 75% (range 41% to 100%) of the initial myocardium, on average, was salvaged. Hence, this line of research can be applied in patient populations, providing a salvageable index for each patient undergoing PCI after acute coronary occlusion, and would potentially increase the knowledge on infarct-related tissue injury.

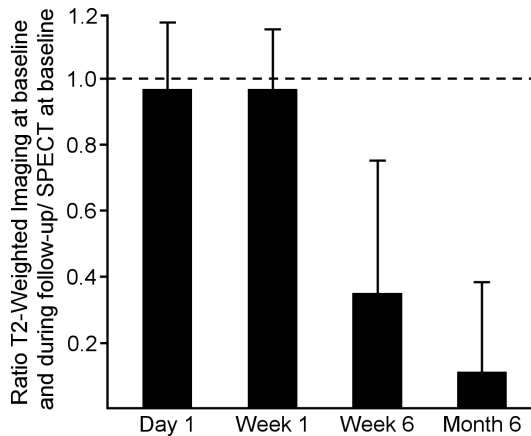


FIGURE 4.4 T2-weighted imaging over time in all patients in relation to perfusion defect at occlusion by myocardial perfusion SPECT. Ratio between T2-imaging and myocardial perfusion SPECT at day 1, week 1, week 6, and month 6 were 0.97 ± 0.20 , 0.97 ± 0.18 , 0.35 ± 0.40 , and 0.11 ± 0.27 , respectively. The presence of edema at 6 months was found in 2 of 9 patients.

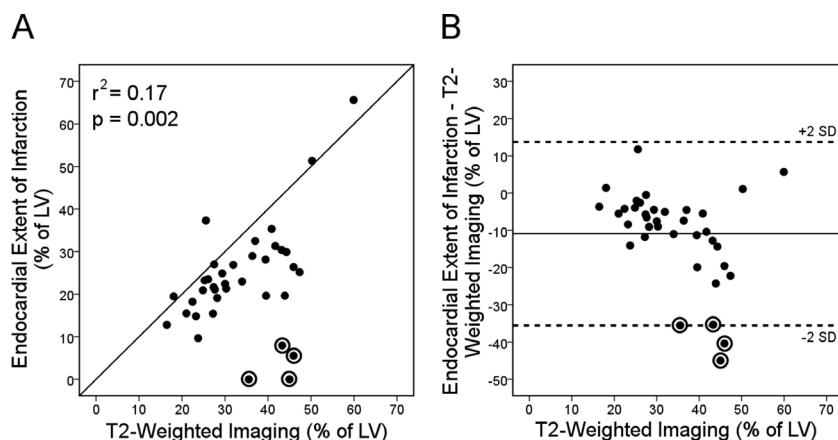


FIGURE 4.5 **A)** MaR by endocardial extent of infarction versus T2-weighted imaging. Solid line = line of identity. **B)** Bland-Altman graph showing the difference between myocardium at risk quantified by endocardial extent of infarction versus T2-weighted imaging. Solid line = mean difference; dashed lines = ± 2 SD. The two patients with an aborted infarction and the two patients with more than 90% myocardial salvage are encircled.

4.2 Endocardial extent of infarction underestimates myocardium at risk (Study II)

Endocardial extent of infarction has been suggested as an alternative method to determine MaR.^{88, 89} The pathophysiological basis for using endocardial extent of infarction to determine MaR is the before mentioned wavefront phenomenon.¹¹

In Study II, the MaR by T2-weighted imaging was $34 \pm 10\%$ (range 18 - 59) of the LV, whereas the MaR by endocardial extent of infarction was $23 \pm 12\%$ (range 0 - 66) of the total LV endocardial surface. There was a weak correlation ($r^2 = 0.17$, $p = 0.002$) between T2-weighted imaging and endocardial extent of infarction for the quantification of MaR (Figure 4.5a) with a bias of $-11 \pm 12\%$ of the LV (Figure 4.5b). This indicates that endocardial extent of infarction underestimates the MaR, and should therefore not be used when an accurate measurement of the MaR is required.

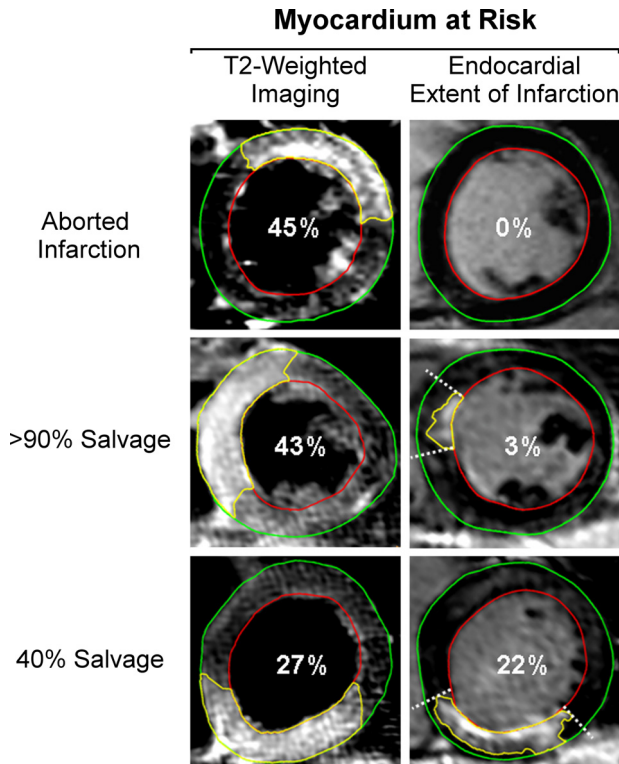


FIGURE 4.6 Short-axis slices at the same ventricular level of T2-weighted imaging and LGE imaging for endocardial extent of infarction in three patients after reperfusion of an acute coronary occlusion. Within the myocardial borders, the affected region is traced in yellow (MaR for T2-weighted imaging and infarction for LGE imaging). The borders of the endocardial extent of infarction are indicated by dashed lines. Within each image the total MaR is given as a percent of left ventricle. The upper panel shows a patient with an aborted infarction, the middle panel a patient with > 90% myocardial salvage and the lower panel a patient with 40% myocardial salvage. Note the difference in size of the MaR by T2-weighted imaging and endocardial extent of infarction for the patient with an aborted infarction and the patient with > 90% myocardial salvage.

When using endocardial extent of infarction for the assessment of MaR, several aspects need to be considered. If early reperfusion is accomplished in the situation of acute coronary occlusion, there might be an absence of LGE on the CMR images, referred to as aborted infarction (Figure 4.6).¹²⁻¹⁵ Consequently, LGE imaging does not allow for determination of MaR in this situation, whereas T2-weighted imaging does. This can in part be explained by the presence of an aborted infarction. In Study II, there were four patients with either an aborted infarction or a very small infarct size (encircled in Figure 4.5), where the MaR by endocardial extent of infarction ranged between 0 and 8% of the LV. In comparison, the MaR assessed by T2-weighted imaging in these patients ranged between 36 and 46% of the LV. Consequently, these differences in MaR also affected determination of myocardial salvage (Figure 4.7). The myocardial salvage assessed by T2-weighted imaging was $58 \pm 22\%$ of LV, which was significantly ($p < 0.001$) higher than the myocardial salvage assessed by endocardial extent of infarction ($45 \pm 23\%$ of LV).

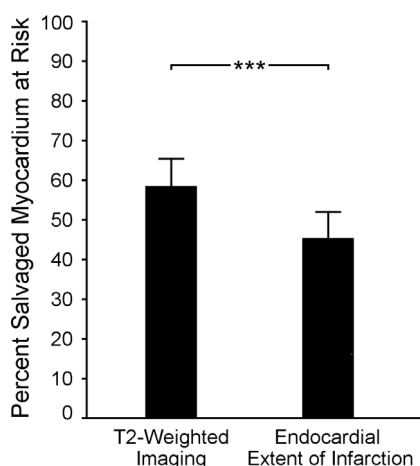


FIGURE 4.7 Mean percent myocardial salvage with T2-weighted imaging and endocardial extent of infarction as the measure for MaR. Myocardial salvage assessed with T2-weighted imaging was significantly higher than when assessed with endocardial extent of infarction. Error bars indicate two standard error of the mean.

In an experimental setting, Fieno *et al.*⁹⁰ showed that the endocardial extent of infarction assessed by LGE imaging might change over time. Furthermore, Engblom *et al.*⁹¹ recently showed that the endocardial extent of LGE significantly decreased during the first week after coronary occlusion. This was explained by a possible decrease in LGE of a viable peri-infarction zone that surrounded the irreversibly injured core of myocytes in the early post-infarction period. This reduction of endocardial LGE implicates a difference in MaR between day one and week one when assessed by CMR. Thus, the endocardial extent of infarction as measured with LGE imaging may change within the first week after coronary occlusion due to initial enhancement of the peri-infarction zone not present at one week. Myocardium at risk by T2-weighted imaging, however, does not change during the first week after infarction, as was shown in Study I.

T2-weighted imaging has been shown to enable distinction between acute and chronic myocardial infarction.⁷³ Hence, MaR can potentially be assessed even in the presence of old infarction. Presence of old infarction, however, disables determination of MaR using endocardial extent of infarction by LGE imaging. Finally, in the case of peri-procedural induction of myocardial infarction, which has been reported to occur in approximately 6% of all patients with non-STEMI undergoing acute reperfusion therapy,⁹² a significant myocardial salvage might be missed if MaR is based on the endocardial extent of a small transmural PCI-induced infarct caused by distal embolization of a small coronary branch.

4.3 Early gadolinium enhancement to assess the myocardium at risk (Study III)

Several experimental studies have demonstrated that the region supplied by the occluded coronary artery, the myocardium at risk, is a major independent variable that determines final infarct size, which in turn is closely related to the clinical outcome.^{36, 37, 93, 94} Thus, feasible and accurate methods for determination of MaR are of significant value, especially in those studies where the effectiveness of acute interventions that aim to reduce final infarct size is analyzed.^{85, 86, 87} In Study III, a region with increased signal intensity by T2-weighted imaging and EGE was observed in all patients, yielding a mean MaR of $29 \pm 11\%$ (range 12 - 65) and $32 \pm 12\%$ (range 8 - 70) of the LV, respectively. Figure 4.8 and Figure 4.9 show examples of the agreement of the MaR by T2-weighted imaging and EGE. There was a strong correlation between the two methods ($r^2 = 0.89$, $p < 0.01$) with a bias of $-3.0 \pm 3.9\%$ of the LV ($p < 0.01$) (Figure 4.10).

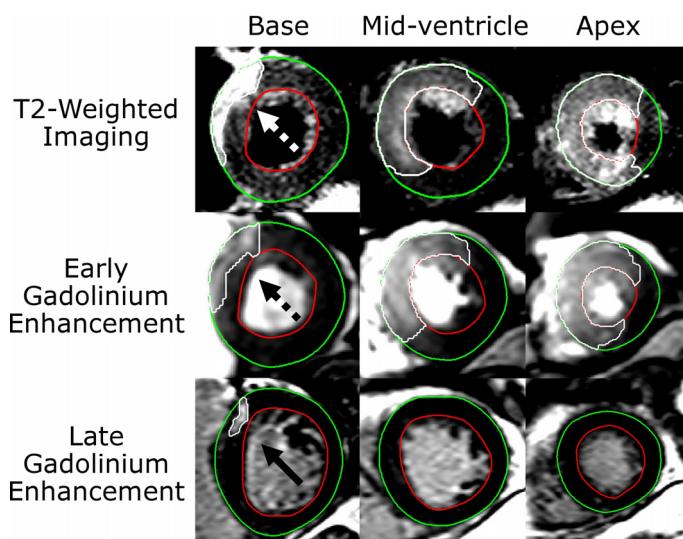


FIGURE 4.8 T2-weighted, early gadolinium enhanced and late gadolinium enhanced short-axis images at the corresponding LV levels in a patient with a reperfused left anterior descending coronary artery occlusion. The epicardium is traced in green and the endocardium is traced in red. The hyperenhanced regions constituting the myocardium at risk (dashed arrows) and the infarcted myocardium (solid arrow) are traced in white. Note the similarity in location and extent of the affected region between T2-weighted imaging and early gadolinium enhancement.

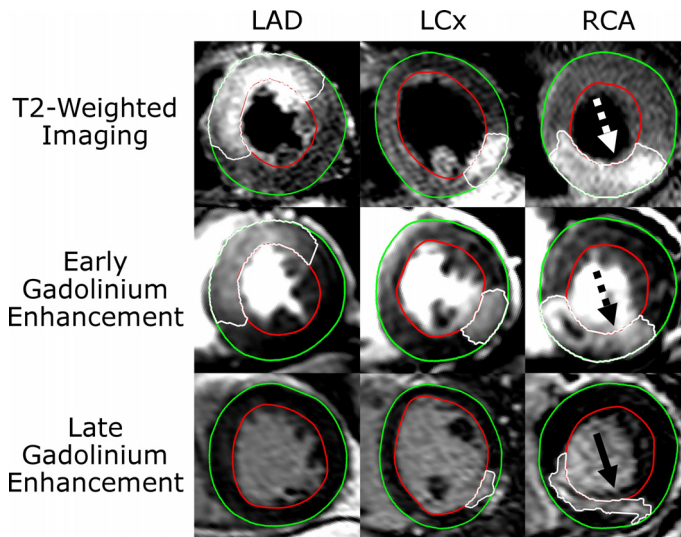


FIGURE 4.9 Corresponding T2-weighted, early gadolinium enhanced and late gadolinium enhanced mid-ventricular short-axis from a patient with an occlusion in the left anterior descending coronary artery (LAD), left circumflex coronary artery (LCx) and the right coronary artery (RCA), respectively. The epicardium is traced in green and the endocardium is traced in red. The hyperenhanced regions constituting the myocardium at risk (dashed arrows) and the infarcted myocardium (solid arrows) are traced in white. Note the similarity in location and extent of the affected region between T2-weighted imaging and early gadolinium enhancement.

The mechanisms behind the enhanced myocardium observed in EGE are not completely known. Steady state free precession (SSFP) cine imaging is normally used to assess myocardial function. Compared to T2-weighted imaging, the contrast seen on the SSFP images is dependent on the ratio between T2-weighting and T1-weighting.⁹⁵ Since the T2/T1 ratio of edematous myocardium is higher than that of normal myocardium,^{96, 97} Green *et al.*⁹⁸ hypothesized that edema should appear brighter on single-shot SSFP images. Indeed, single-shot SSFP proved to be feasible to detect myocardial edema with a moderate sensitivity and high specificity. More recently, early gadolinium enhanced SSFP (EGE) has been introduced as a method to assess MaR, which was validated against myocardial perfusion SPECT.⁹⁹ This method is based on acquisition of time resolved SSFP images early after injection of a gadolinium-based contrast agent. In the presence of paramagnetic gadolinium, the T1 relaxation time for the surrounding tissue is shortened. This is utilized for infarct visualization in T1-weighted LGE imaging, where the concentration of an extracellular gadolinium-based contrast agent is increased due to an increased distribution volume in irreversibly injured myocardium.^{82, 83, 100, 101} It has, however, also been shown that reversibly injured myocardium has an increased distribution volume after an ischemic episode.^{82, 83} Hence, it is possible that the T2/T1 ratio in the entire MaR, including both reversible and irreversible injured myocardium, is affected by the presence of gadolinium. This might explain the increased signal intensity in the MaR as seen by EGE.

Another possible mechanism behind EGE is the altered wash-in/wash-out kinetics after an ischemic episode, affecting the early distribution of gadolinium.¹⁰⁴⁻¹⁰⁷ Kim *et al.*¹⁰⁸ found no significant difference in wash-in time between remote, adjacent and infarcted myocardium. There was, however, a significant difference in wash-out time between these regions, which might explain why there is transmural hyperenhancement within the MaR in EGE images.

The clinical usefulness of the present study is mainly that there are several advantages of having access to more than one method for determination of MaR by CMR imaging. Even though T2-weighted imaging is promising for assessment of MaR, this technique still has certain limitations, such as difficulties in distinguishing blood pool from myocardium, especially in the apical parts of the left ventricle where hypokinesia and trabeculation causes stagnant blood flow.¹⁰² Likewise, reduced cardiac motion decreases the likelihood of misregistration between dark-blood preparation and imaging phases.¹⁰³ Therefore, hypokinetic myocardium may appear hyperintense in comparison with normal regions that have suffered signal loss because of through-plane motion. In addition, artifacts caused by signal dropout are more common at higher heart rates. Finally, the

signal-to-noise ratio is often low and can vary between slices in the same patient, making automatic definition of the MaR difficult and operator-dependent. Early gadolinium enhanced SSFP imaging does not show the artefacts encountered with T2-weighted imaging and can therefore be used as an alternative method to assess the MaR in those patients where artefacts are present on the T2-weighted images. Furthermore, EGE could be the method of choice when limited time for scanning is available, due to heavy clinical load or an unstable patient. In such a situation, gadolinium can be injected prior to the examination and the imaging protocol can be shortened, since LV dimensions/function and MaR can be assessed from the same set of images. On the other hand, T2-weighted imaging can be performed in those patients where administration of a gadolinium-based contrast agent is contraindicated.

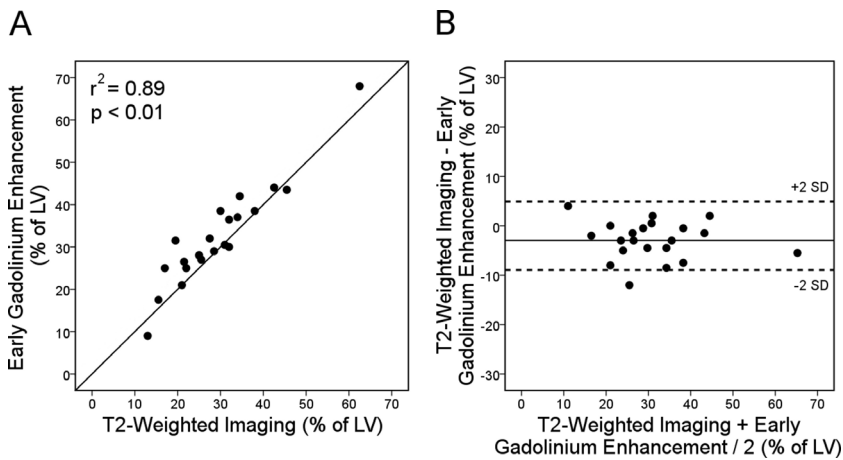


FIGURE 4.10 Relationship between T2-weighted imaging and early gadolinium enhancement for myocardium at risk. **A)** MaR by T2-weighted imaging versus early gadolinium enhancement (EGE). Solid line = line of identity. **B)** Bland-Altman graph. The difference between T2-weighted imaging and EGE was $-3.0 \pm 3.9\%$. Solid line = mean difference; dashed lines = ± 2 SD.

4.4 *Ex vivo* T2-weighted imaging for MaR in the presence of gadolinium (Study IV)

In experimental models, the presence of edema in ischemic myocardium has been observed in *in vivo* studies with the use of T2-weighted imaging.^{12, 74} There are, however, only few studies that validated T2-weighted imaging for measuring MaR *ex vivo*.⁷⁶ Furthermore, *ex vivo* T2-weighted imaging has never been compared against myocardial perfusion SPECT.

In humans (Study I), we validated T2-weighted imaging against MaR assessed by myocardial perfusion SPECT, showing a strong correlation between the two methods ($r^2 = 0.70$) with a small bias of $-2.3 \pm 5.7\%$. Study IV showed a strong correlation ($r^2 = 0.70$, $p < 0.01$) and a small bias $2.1 \pm 4.2\%$ when *ex vivo* T2-weighted imaging, both with and without the presence of gadolinium, was compared to myocardial perfusion SPECT (Figure 4.11). The current findings are also in accordance with previous experimental studies where the MaR by T2-weighted imaging was compared against microspheres and fluorescein.^{74, 76} Aletras *et al.*⁷⁴ found a small bias between the two methods with a slightly larger standard deviation, whereas Garcia-Dorado *et al.*⁷⁶ also showed a small overestimation of the MaR by T2-weighted imaging. The correlation between T2-weighted imaging and myocardial perfusion SPECT remained significant when the animals were separated into a group without the presence of gadolinium ($r^2 = 0.78$, $p < 0.01$; bias $4.3 \pm 2.9\%$) and a group with the presence of gadolinium ($r^2 = 0.63$, $p < 0.01$; $0.6 \pm 4.4\%$). An example of a comparison between T2-weighted imaging and myocardial perfusion SPECT without the presence of gadolinium can be seen in Figure 4.12.

In a standard clinical protocol, a patient is injected with a gadolinium-based contrast agent for infarct visualization by CMR. The gadolinium is distributed in the myocardium proportional to the amount of extracellular space in the tissue.⁸² In regions with ischemic injury, the distribution volume is increased⁸³ and the presence of gadolinium affects the T1 tissue properties in this region.⁶⁹ However, gadolinium also affects the T2 tissue properties of the myocardium that are normally utilized for visualization of edema by T2-weighted imaging. The triple inversion-recovery sequence (T2-STIR), used in standard clinical protocols, is particularly sensitive to the presence of gadolinium and imaging is therefore performed prior to administration of gadolinium to avoid signal loss. This is, however, difficult in an *ex vivo* experimental model since gadolinium has to be administered before sacrificing the animal to enable assessment of myocardial infarction. The effect of gadolinium on T2-STIR is shown in Figure 4.13. Without the presence of gadolinium, a distinct hyperintense region can be seen on the T2-STIR image, whereas in the presence of gadolinium, no hyper-

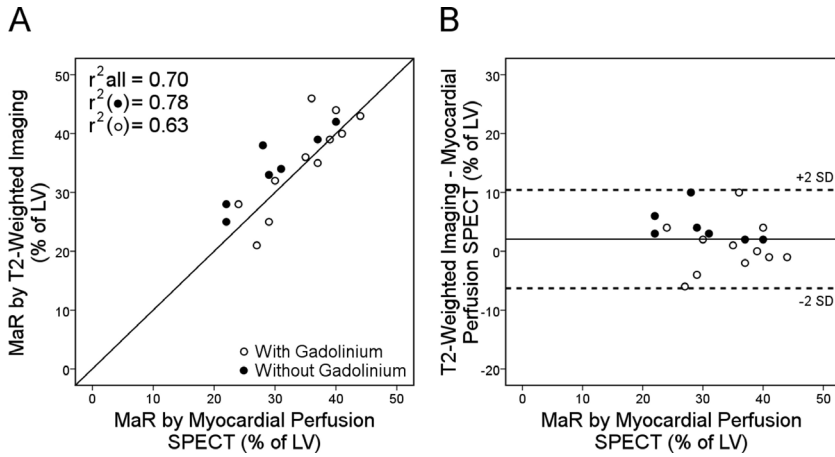


FIGURE 4.11 **A)** Relationship between T2-weighted imaging and myocardial perfusion SPECT for assessment of MaR, both with and without the presence of gadolinium. Solid line = line of identity. **B)** The limits of agreement between the two measures of MaR. The difference between the two methods was $2.1 \pm 4.2\%$. Solid line = mean difference; dashed lines = ± 2 SD.

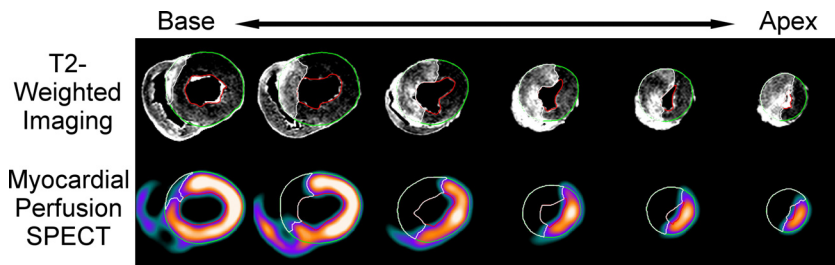


FIGURE 4.12 Short-axis slices at the same ventricular level for T2-weighted imaging and myocardial perfusion SPECT in a pig subjected to 30 minutes of coronary artery occlusion. The epicardium is traced in green, the endocardium is traced in red, and the MaR is traced in white. In this particular pig, the MaR was 33% by T2-weighted imaging and 29% by myocardial perfusion SPECT.

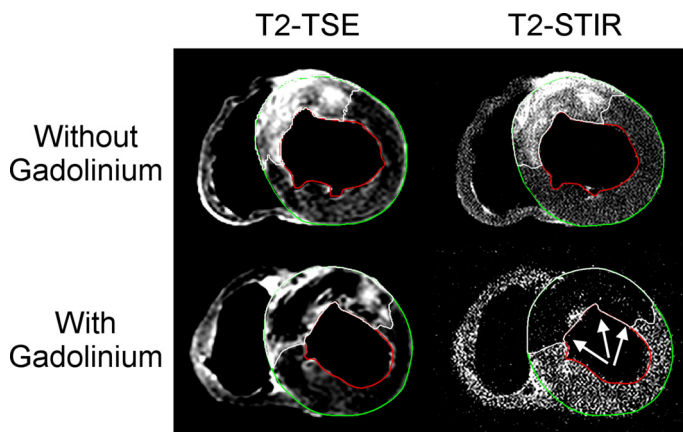


FIGURE 4.13 Short-axis T2-TSE and T2-STIR images in one pig before injection of gadolinium and in one pig after injection of gadolinium. The epicardium is traced in green, the endocardium is traced in red, and the corresponding MaR is traced in white. A hyperintense region can be seen in both T2-TSE and T2-STIR without the presence of gadolinium. Note that no hyperintense region can be seen on the T2-STIR image due to the presence of gadolinium (white arrows), whereas the T2-TSE image clearly shows both hyperintense and hypointense regions within the MaR.

enhancement can be seen in the myocardium. There was, however, a hypointense region that corresponded to the MaR seen by T2-TSE (double inversion-recovery sequence) and myocardial perfusion SPECT (white arrows in Figure 4.14). In comparison, the T2-TSE images after injection of gadolinium had both hyperintense and hypointense regions within the MaR. The hypointense regions were shown to be closely related to the infarcted regions seen by TTC-staining, whereas no myocardial infarction could be seen by TTC-staining in those regions showing a hyperintense region by T2-TSE imaging (Figure 4.14). Thus, T2-TSE can therefore be used to assess myocardial salvage in an experimental model since this method enables determination of MaR after administration of gadolinium used to assess infarct size.

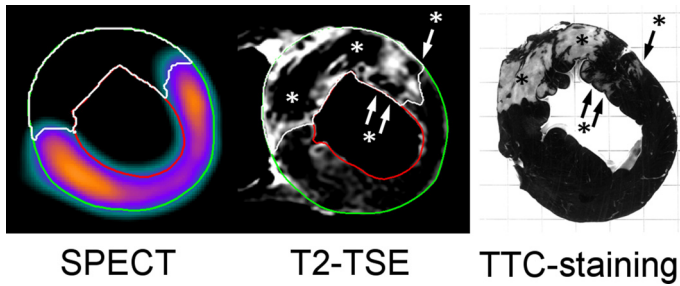


FIGURE 4.14 Corresponding mid-ventricular short-axis slices from a pig subjected to 30 minutes of coronary artery occlusion. The MaR is shown in white on the myocardial perfusion SPECT image (left) and on the T2-weighted image (middle) after injection of a gadolinium-based contrast agent. The infarcted myocardium can be seen as the pale areas on the TTC-staining image (right). Note that the hypointense regions on the T2-weighted image correspond well with the infarcted regions by TTC-staining, as indicated by *, whereas no infarct can be seen in the areas with hyperintense signal on the T2-weighted image.

Chapter 5

Conclusions

This thesis has investigated and validated different CMR techniques to quantitatively and qualitatively assess the myocardium at risk. The major conclusions of each study were:

- I. T2-weighted imaging performed up to 1 week after reperfusion can accurately determine myocardium at risk as it was before opening of the occluded artery in patients with acute coronary occlusion. Furthermore, the outcome of cardioprotective strategies can be assessed within one CMR session by determining the amount of myocardial salvage.
- II. The endocardial extent of infarction as assessed by late gadolinium enhanced CMR underestimates myocardium at risk in comparison to T2-weighted imaging, especially in patients with early reperfusion and aborted myocardial infarction.
- III. There is a strong agreement between myocardium at risk assessed by T2-weighted imaging and myocardium at risk assessed by early gadolinium enhancement in patients with reperfused acute myocardial infarction 1 week after the acute event. Thus, both methods can be used to determine MaR and subsequently myocardial salvage at this point in time.
- IV. T2-weighted imaging can be used to determine the myocardium at risk in an *ex vivo* experimental model, both with and without the presence of gadolinium. Thus, CMR can be used to assess myocardial salvage in experimental studies without the use of myocardial perfusion SPECT.

Bibliography

- [1] Roger VL, Go AS, Lloyd-Jones DM, Adams RJ, Berry JD, Brown TM, Carnethon MR, Dai S, de Simone G, et al. Heart disease and stroke statistics--2011 update: a report from the American Heart Association. *Circulation*, 123(4): e18-e209, 2011.
- [2] Myocardial Infarctions in Sweden, 1987-2007. *www.socialstyrelsen.se*, 2009.
- [3] Gould KL, Lipscomb K, Hamilton GW. Physiologic basis for assessing critical coronary stenosis. Instantaneous flow response and regional distribution during coronary hyperemia as measures of coronary flow reserve. *Am J Cardiol*, 33(1): 87-94, 1974.
- [4] Farber JL, Chien KR, Mittnacht S, Jr. Myocardial ischemia: the pathogenesis of irreversible cell injury in ischemia. *Am J Pathol*, 102(2): 271-281, 1981.
- [5] Kristian T, Siesjö BK. Calcium in ischemic cell death. *Stroke*, 29(3): 705-718, 1998.
- [6] Duncan CJ. The role of phospholipase A2 in calcium-induced damage in cardiac and skeletal muscle. *Cell Tissue Res*, 253(2): 457-462, 1988.
- [7] Gissel H. The role of Ca²⁺ in muscle cell damage. *Ann N Y Acad Sci*, 1066: 166-180, 2005.
- [8] Misra MK, Sarwat M, Bhakuni P, Tuteja R, Tuteja N. Oxidative stress and ischemic myocardial syndromes. *Med Sci Monit*, 15(10): RA209-219, 2009.
- [9] Levraut J, Iwase H, Shao ZH, Vanden Hoek TL, Schumacker PT. Cell death during ischemia: relationship to mitochondrial depolarization and ROS generation. *Am J Physiol Heart Circ Physiol*, 284(2): H549-558, 2003.
- [10] Antman EM. Time is muscle: translation into practice. *J Am Coll Cardiol*, 52(15): 1216-1221, 2008.
- [11] Reimer KA, Lowe JE, Rasmussen MM, Jennings RB. The wavefront phenomenon of ischemic cell death. 1. Myocardial infarct size vs duration of coronary occlusion in dogs. *Circulation*, 56(5): 786-794, 1977.

- [12] Abdel-Aty H, Cocker M, Meek C, Tyberg JV, Friedrich MG. Edema as a very early marker for acute myocardial ischemia: a cardiovascular magnetic resonance study. *J Am Coll Cardiol*, 53(14): 1194-1201, 2009.
- [13] Cury RC, Shash K, Nagurney JT, Rosito G, Shapiro MD, Nomura CH, Abbata S, Bamberg F, Ferencik M, et al. Cardiac magnetic resonance with T2-weighted imaging improves detection of patients with acute coronary syndrome in the emergency department. *Circulation*, 118(8): 837-844, 2008.
- [14] Lamfers EJ, Hooghoudt TE, Hertzberger DP, Schut A, Stolwijk PW, Verheugt FW. Abortion of acute ST segment elevation myocardial infarction after reperfusion: incidence, patients' characteristics, and prognosis. *Heart*, 89(5): 496-501, 2003.
- [15] Weaver WD, Cerqueira M, Hallstrom AP, Litwin PE, Martin JS, Kudenchuk PJ, Eisenberg M. Prehospital-initiated vs hospital-initiated thrombolytic therapy. The Myocardial Infarction Triage and Intervention Trial. *JAMA*, 270(10): 1211-1216, 1993.
- [16] Hedstrom E, Engblom H, Frogner F, Astrom-Olsson K, Ohlin H, Jovinge S, Arheden H. Infarct evolution in man studied in patients with first-time coronary occlusion in comparison to different species - implications for assessment of myocardial salvage. *J Cardiovasc Magn Reson*, 11: 38, 2009.
- [17] Boersma E, Maas AC, Deckers JW, Simoons ML. Early thrombolytic treatment in acute myocardial infarction: reappraisal of the golden hour. *Lancet*, 348(9030): 771-775, 1996.
- [18] Weaver WD. Time to thrombolytic treatment: factors affecting delay and their influence on outcome. *J Am Coll Cardiol*, 25(7 Suppl): 3S-9S, 1995.
- [19] Kushner FG, Hand M, Smith SC, Jr., King SB, 3rd, Anderson JL, Antman EM, Bailey SR, Bates ER, Blankenship JC, et al. 2009 Focused Updates: ACC/AHA Guidelines for the Management of Patients With ST-Elevation Myocardial Infarction (updating the 2004 Guideline and 2007 Focused Update) and ACC/AHA/SCAI Guidelines on Percutaneous Coronary Intervention (updating the 2005 Guideline and 2007 Focused Update): a report of the American College of Cardiology Foundation/American Heart Association Task Force on Practice Guidelines. *Circulation*, 120(22): 2271-2306, 2009.
- [20] Rathore SS, Curtis JP, Chen J, Wang Y, Nallamothu BK, Epstein AJ, Krumholz HM. Association of door-to-balloon time and mortality in patients admitted to hospital with ST elevation myocardial infarction: national cohort study. *BMJ*, 338: b1807, 2009.
- [21] Murry CE, Jennings RB, Reimer KA. Preconditioning with ischemia: a delay of lethal cell injury in ischemic myocardium. *Circulation*, 74(5): 1124-1136, 1986.

- [22] Li GC, Vasquez JA, Gallagher KP, Lucchesi BR. Myocardial protection with preconditioning. *Circulation*, 82(2): 609-619, 1990.
- [23] Li YW, Whittaker P, Kloner RA. The transient nature of the effect of ischemic preconditioning on myocardial infarct size and ventricular arrhythmia. *Am Heart J*, 123(2): 346-353, 1992.
- [24] Schott RJ, Rohmann S, Braun ER, Schaper W. Ischemic preconditioning reduces infarct size in swine myocardium. *Circ Res*, 66(4): 1133-1142, 1990.
- [25] Thornton J, Striplin S, Liu GS, Swafford A, Stanley AW, Van Winkle DM, Downey JM. Inhibition of protein synthesis does not block myocardial protection afforded by preconditioning. *Am J Physiol*, 259(6 Pt 2): H1822-1825, 1990.
- [26] Deutsch E, Berger M, Kussmaul WG, Hirshfeld JW, Jr., Herrmann HC, Laskey WK. Adaptation to ischemia during percutaneous transluminal coronary angioplasty. Clinical, hemodynamic, and metabolic features. *Circulation*, 82(6): 2044-2051, 1990.
- [27] Kloner RA, Yellon D. Does ischemic preconditioning occur in patients? *J Am Coll Cardiol*, 24(4): 1133-1142, 1994.
- [28] Tyagi P, Tayal G. Ischemic preconditioning of myocardium. *Acta Pharmacol Sin*, 23(10): 865-870, 2002.
- [29] Murry CE, Richard VJ, Reimer KA, Jennings RB. Ischemic preconditioning slows energy metabolism and delays ultrastructural damage during a sustained ischemic episode. *Circ Res*, 66(4): 913-931, 1990.
- [30] Maxwell MP, Hearse DJ, Yellon DM. Species variation in the coronary collateral circulation during regional myocardial ischaemia: a critical determinant of the rate of evolution and extent of myocardial infarction. *Cardiovasc Res*, 21(10): 737-746, 1987.
- [31] Schaper W, Gorge G, Winkler B, Schaper J. The collateral circulation of the heart. *Prog Cardiovasc Dis*, 31(1): 57-77, 1988.
- [32] Kolibash AJ, Bush CA, Wepsic RA, Schroeder DP, Tetelman MR, Lewis RP. Coronary collateral vessels: spectrum of physiologic capabilities with respect to providing rest and stress myocardial perfusion, maintenance of left ventricular function and protection against infarction. *Am J Cardiol*, 50(2): 230-238, 1982.
- [33] Charney R, Cohen M. The role of the coronary collateral circulation in limiting myocardial ischemia and infarct size. *Am Heart J*, 126(4): 937-945, 1993.
- [34] Williams DO, Amsterdam EA, Miller RR, Mason DT. Functional significance of coronary collateral vessels in patients with acute myocardial infarction: relation to

- pump performance, cardiogenic shock and survival. *Am J Cardiol*, 37(3): 345-351, 1976.
- [35] Jennings RB, Sommers HM, Smyth GA, Flack HA, Linn H. Myocardial necrosis induced by temporary occlusion of a coronary artery in the dog. *Arch Pathol*, 70:68-78, 1960.
- [36] Lee JT, Ideker RE, Reimer KA. Myocardial infarct size and location in relation to the coronary vascular bed at risk in man. *Circulation*, 64(3): 526-534, 1981.
- [37] Lowe JE, Reimer KA, Jennings RB. Experimental infarct size as a function of the amount of myocardium at risk. *Am J Pathol*, 90(2): 363-379, 1978.
- [38] Kloner RA, Bolli R, Marban E, Reinlib L, Braunwald E. Medical and cellular implications of stunning, hibernation, and preconditioning: an NHLBI workshop. *Circulation*, 97(18): 1848-1867, 1998.
- [39] Thygesen K, Alpert JS, White HD. Universal definition of myocardial infarction. *Eur Heart J*, 28(20): 2525-2538, 2007.
- [40] Bruce RA, Hornsten TR. Exercise stress testing in evaluation of patients with ischemic heart disease. *Prog Cardiovasc Dis*, 11(5): 371-390, 1969.
- [41] Hendel RC, Berman DS, Di Carli MF, Heidenreich PA, Henkin RE, Pellikka PA, Pohost GM, Williams KA. ACCF/ ASNC/ ACR/ AHA/ ASE/ SCCT/ SCMR/ SNM 2009 appropriate use criteria for cardiac radionuclide imaging: a report of the American College of Cardiology Foundation Appropriate Use Criteria Task Force, the American Society of Nuclear Cardiology, the American College of Radiology, the American Heart Association, the American Society of Echocardiography, the Society of Cardiovascular Computed Tomography, the Society for Cardiovascular Magnetic Resonance, and the Society of Nuclear Medicine. *Circulation*, 119(22): e561-587, 2009.
- [42] Gebker R, Jahnke C, Manka R, Hamdan A, Schnackenburg B, Fleck E, Paetsch I. Additional value of myocardial perfusion imaging during dobutamine stress magnetic resonance for the assessment of coronary artery disease. *Circ Cardiovasc Imaging*, 1(2): 122-130, 2008.
- [43] Keeley EC, Boura JA, Grines CL. Primary angioplasty versus intravenous thrombolytic therapy for acute myocardial infarction: a quantitative review of 23 randomised trials. *Lancet*, 361(9351): 13-20, 2003.
- [44] Stenestrand U, Lindback J, Wallentin L. Long-term outcome of primary percutaneous coronary intervention vs prehospital and in-hospital thrombolysis for patients with ST-elevation myocardial infarction. *JAMA*, 296(14): 1749-1756, 2006.

- [45] An international randomized trial comparing four thrombolytic strategies for acute myocardial infarction. The GUSTO investigators. *N Engl J Med*, 329(10): 673-682, 1993.
- [46] Coronary artery bypass surgery versus percutaneous coronary intervention with stent implantation in patients with multivessel coronary artery disease (the Stent or Surgery trial): a randomised controlled trial. *Lancet*, 360(9338): 965-970, 2002.
- [47] Serruys PW, Morice MC, Kappetein AP, Colombo A, Holmes DR, Mack MJ, Stahle E, Feldman TE, van den Brand M, et al. Percutaneous coronary intervention versus coronary-artery bypass grafting for severe coronary artery disease. *N Engl J Med*, 360(10): 961-972, 2009.
- [48] Van de Werf F, Bax J, Betriu A, Blomstrom-Lundqvist C, Crea F, Falk V, Filippatos G, Fox K, Huber K, et al. Management of acute myocardial infarction in patients presenting with persistent ST-segment elevation: the Task Force on the Management of ST-Segment Elevation Acute Myocardial Infarction of the European Society of Cardiology. *Eur Heart J*, 29(23): 2909-2945, 2008.
- [49] Buch P, Rasmussen S, Gislason GH, Rasmussen JN, Kober L, Gadsboll N, Stender S, Madsen M, Torp-Pedersen C, et al. Temporal decline in the prognostic impact of a recurrent acute myocardial infarction 1985 to 2002. *Heart*, 93(2): 210-215, 2007.
- [50] Dobrucki LW, Sinusas AJ. Imaging angiogenesis. *Curr Opin Biotechnol*, 18(1): 90-96, 2007.
- [51] Anderson JL, Adams CD, Antman EM, Bridges CR, Califf RM, Casey DE, Jr., Chavey WE, 2nd, Fesmire FM, Hochman JS, et al. ACC/AHA 2007 guidelines for the management of patients with unstable angina/non ST-elevation myocardial infarction: a report of the American College of Cardiology/American Heart Association Task Force on Practice Guidelines (Writing Committee to Revise the 2002 Guidelines for the Management of Patients With Unstable Angina/Non ST-Elevation Myocardial Infarction): developed in collaboration with the American College of Emergency Physicians, the Society for Cardiovascular Angiography and Interventions, and the Society of Thoracic Surgeons: endorsed by the American Association of Cardiovascular and Pulmonary Rehabilitation and the Society for Academic Emergency Medicine. *Circulation*, 116(7): e148-304, 2007.
- [52] Gibbons RJ, Abrams J, Chatterjee K, Daley J, Deedwania PC, Douglas JS, Ferguson TB, Jr., Fihn SD, Fraker TD, Jr., et al. ACC/AHA 2002 guideline update for the management of patients with chronic stable angina--summary article: a report of the American College of Cardiology/American Heart Association Task Force on Practice Guidelines (Committee on the Management of Patients With Chronic Stable Angina). *Circulation*, 107(1): 149-158, 2003.

- [53] Hendel RC, Wackers FJ, Berman DS, Ficaro E, DePuey EG, Klein L, Cerqueira M. American Society of Nuclear Cardiology consensus statement: Reporting of radionuclide myocardial perfusion imaging studies. *J Nucl Cardiol*, 13(6): e152-156, 2006.
- [54] Hesse B, Tagil K, Cuocolo A, Anagnostopoulos C, Bardies M, Bax J, Bengel F, Busemann Sokole E, Davies G, et al. EANM/ESC procedural guidelines for myocardial perfusion imaging in nuclear cardiology. *Eur J Nucl Med Mol Imaging*, 32(7): 855-897, 2005.
- [55] Ceriani L, Verna E, Giovanella L, Bianchi L, Roncari G, Tarolo GL. Assessment of myocardial area at risk by technetium-99m sestamibi during coronary artery occlusion: comparison between three tomographic methods of quantification. *Eur J Nucl Med*, 23(1): 31-39, 1996.
- [56] Sinusas AJ, Trautman KA, Bergin JD, Watson DD, Ruiz M, Smith WH, Beller GA. Quantification of area at risk during coronary occlusion and degree of myocardial salvage after reperfusion with technetium-99m methoxyisobutyl isonitrile. *Circulation*, 82(4): 1424-1437, 1990.
- [57] Gibbons RJ, Miller TD, Christian TF. Infarct size measured by single photon emission computed tomographic imaging with (99m)Tc-sestamibi: A measure of the efficacy of therapy in acute myocardial infarction. *Circulation*, 101(1): 101-108, 2000.
- [58] Wackers FJ. Comparison of thallium-201 and technetium-99m methoxyisobutyl isonitrile. *Am J Cardiol*, 70(14): 30E-34E, 1992.
- [59] Beller GA, Watson DD, Ackell P, Pohost GM. Time course of thallium-201 redistribution after transient myocardial ischemia. *Circulation*, 61(4): 791-797, 1980.
- [60] Garcia EV. SPECT attenuation correction: an essential tool to realize nuclear cardiology's manifest destiny. *J Nucl Cardiol*, 14(1): 16-24, 2007.
- [61] Kaufmann PA, Di Carli MF. Hybrid SPECT/CT and PET/CT imaging: the next step in noninvasive cardiac imaging. *Semin Nucl Med*, 39(5): 341-347, 2009.
- [62] Faber TL, Cooke CD, Folks RD, Vansant JP, Nichols KJ, DePuey EG, Pettigrew RI, Garcia EV. Left ventricular function and perfusion from gated SPECT perfusion images: an integrated method. *J Nucl Med*, 40(4): 650-659, 1999.
- [63] Germano G, Kavanagh PB, Waechter P, Areeda J, Van Kriekinge S, Sharir T, Lewin HC, Berman DS. A new algorithm for the quantitation of myocardial perfusion SPECT. I: technical principles and reproducibility. *J Nucl Med*, 41(4): 712-719, 2000.
- [64] Persson E, Carlsson M, Palmer J, Pahlm O, Arheden H. Evaluation of left ventricular volumes and ejection fraction by automated gated myocardial SPECT

- versus cardiovascular magnetic resonance. *Clin Physiol Funct Imaging*, 25(3): 135-141, 2005.
- [65] Soneson H, Ubachs JF, Ugander M, Arheden H, Heiberg E. An improved method for automatic segmentation of the left ventricle in myocardial perfusion SPECT. *J Nucl Med*, 50(2): 205-213, 2009.
- [66] Bitar R, Leung G, Perng R, Tadros S, Moody AR, Sarrazin J, McGregor C, Christakis M, Symons S, et al. MR pulse sequences: what every radiologist wants to know but is afraid to ask. *Radiographics*, 26(2): 513-537, 2006.
- [67] Pooley RA. AAPM/RSNA physics tutorial for residents: fundamental physics of MR imaging. *Radiographics*, 25(4): 1087-1099, 2005.
- [68] Ridgway JP. Cardiovascular magnetic resonance physics for clinicians: part I. *J Cardiovasc Magn Reson*, 12: 71, 2010.
- [69] Weinmann HJ, Brasch RC, Press WR, Wesbey GE. Characteristics of gadolinium-DTPA complex: a potential NMR contrast agent. *AJR Am J Roentgenol*, 142(3): 619-624, 1984.
- [70] Soneson H, Engblom H, Hedstrom E, Bouvier F, Sorensson P, Pernow J, Arheden H, Heiberg E. An automatic method for quantification of myocardium at risk from myocardial perfusion SPECT in patients with acute coronary occlusion. *J Nucl Cardiol*, 17(5): 831-840, 2010.
- [71] Heiberg E, Sjogren J, Ugander M, Carlsson M, Engblom H, Arheden H. Design and validation of Segment--freely available software for cardiovascular image analysis. *BMC Med Imaging*, 10: 1, 2010.
- [72] Heiberg E, Ugander M, Engblom H, Gotberg M, Olivecrona GK, Erlinge D, Arheden H. Automated quantification of myocardial infarction from MR images by accounting for partial volume effects: animal, phantom, and human study. *Radiology*, 246(2): 581-588, 2008.
- [73] Abdel-Aty H, Zagrosek A, Schulz-Menger J, Taylor AJ, Messroghli D, Kumar A, Gross M, Dietz R, Friedrich MG. Delayed enhancement and T2-weighted cardiovascular magnetic resonance imaging differentiate acute from chronic myocardial infarction. *Circulation*, 109(20): 2411-2416, 2004.
- [74] Aletras AH, Tilak GS, Natanzon A, Hsu LY, Gonzalez FM, Hoyt RF, Jr., Arai AE. Retrospective determination of the area at risk for reperfused acute myocardial infarction with T2-weighted cardiac magnetic resonance imaging: histopathological and displacement encoding with stimulated echoes (DENSE) functional validations. *Circulation*, 113(15): 1865-1870, 2006.
- [75] Friedrich MG, Abdel-Aty H, Taylor A, Schulz-Menger J, Messroghli D, Dietz R. The salvaged area at risk in reperfused acute myocardial infarction as visualized by cardiovascular magnetic resonance. *J Am Coll Cardiol*, 51(16): 1581-1587, 2008.

- [76] Garcia-Dorado D, Oliveras J, Gili J, Sanz E, Perez-Villa F, Barrabes J, Carreras MJ, Solares J, Soler-Soler J. Analysis of myocardial oedema by magnetic resonance imaging early after coronary artery occlusion with or without reperfusion. *Cardiovasc Res*, 27(8): 1462-1469, 1993.
- [77] Tilak GS, Hsu LY, Hoyt RF, Jr., Arai AE, Aletras AH. In vivo T2-weighted magnetic resonance imaging can accurately determine the ischemic area at risk for 2-day-old nonreperfused myocardial infarction. *Invest Radiol*, 43(1): 7-15, 2008.
- [78] Stork A, Lund GK, Muellerleile K, Bansmann PM, Nolte-Ernsting C, Kemper J, Begemann PG, Adam G. Characterization of the peri-infarction zone using T2-weighted MRI and delayed-enhancement MRI in patients with acute myocardial infarction. *Eur Radiol*, 16(10): 2350-2357, 2006.
- [79] Fishbein MC, Maclean D, Maroko PR. The histopathologic evolution of myocardial infarction. *Chest*, 73(6): 843-849, 1978.
- [80] Steenbergen C, Hill ML, Jennings RB. Volume regulation and plasma membrane injury in aerobic, anaerobic, and ischemic myocardium in vitro. Effects of osmotic cell swelling on plasma membrane integrity. *Circ Res*, 57(6): 864-875, 1985.
- [81] Willerson JT, Scales F, Mukherjee A, Platt M, Templeton GH, Fink GS, Buja LM. Abnormal myocardial fluid retention as an early manifestation of ischemic injury. *Am J Pathol*, 87(1): 159-188, 1977.
- [82] Arheden H, Saeed M, Higgins CB, Gao DW, Bremerich J, Wyttenbach R, Dae MW, Wendland MF. Measurement of the distribution volume of gadopentetate dimeglumine at echo-planar MR imaging to quantify myocardial infarction: comparison with 99mTc-DTPA autoradiography in rats. *Radiology*, 211(3): 698-708, 1999.
- [83] Arheden H, Saeed M, Higgins CB, Gao DW, Ursell PC, Bremerich J, Wyttenbach R, Dae MW, Wendland MF. Reperfused rat myocardium subjected to various durations of ischemia: estimation of the distribution volume of contrast material with echo-planar MR imaging. *Radiology*, 215(2): 520-528, 2000.
- [84] Garcia-Dorado D, Oliveras J. Myocardial oedema: a preventable cause of reperfusion injury? *Cardiovasc Res*, 27(9): 1555-1563, 1993.
- [85] Gotberg M, Olivecrona GK, Engblom H, Ugander M, van der Pals J, Heiberg E, Arheden H, Erlinge D. Rapid short-duration hypothermia with cold saline and endovascular cooling before reperfusion reduces microvascular obstruction and myocardial infarct size. *BMC Cardiovasc Disord*, 8: 7, 2008.
- [86] van der Pals J, Koul S, Andersson P, Gotberg M, Ubachs JF, Kanski M, Arheden H, Olivecrona GK, Larsson B, et al. Treatment with the C5a receptor antagonist

- ADC-1004 reduces myocardial infarction in a porcine ischemia-reperfusion model. *BMC Cardiovasc Disord*, 10: 45, 2010.
- [87] Ibanez B, Prat-Gonzalez S, Speidl WS, Vilahur G, Pinero A, Cimmino G, Garcia MJ, Fuster V, Sanz J, et al. Early metoprolol administration before coronary reperfusion results in increased myocardial salvage: analysis of ischemic myocardium at risk using cardiac magnetic resonance. *Circulation*, 115(23): 2909-2916, 2007.
- [88] Ortiz-Perez JT, Meyers SN, Lee DC, Kansal P, Klocke FJ, Holly TA, Davidson CJ, Bonow RO, Wu E. Angiographic estimates of myocardium at risk during acute myocardial infarction: validation study using cardiac magnetic resonance imaging. *Eur Heart J*, 28(14): 1750-1758, 2007.
- [89] Wright J, Adriaenssens T, Dymarkowski S, Desmet W, Bogaert J. Quantification of myocardial area at risk with T2-weighted CMR: comparison with contrast-enhanced CMR and coronary angiography. *JACC Cardiovasc Imaging*, 2(7): 825-831, 2009.
- [90] Fieno DS, Hillenbrand HB, Rehwald WG, Harris KR, Decker RS, Parker MA, Klocke FJ, Kim RJ, Judd RM. Infarct resorption, compensatory hypertrophy, and differing patterns of ventricular remodeling following myocardial infarctions of varying size. *J Am Coll Cardiol*, 43(11): 2124-2131, 2004.
- [91] Engblom H, Hedstrom E, Heiberg E, Wagner GS, Pahlm O, Arheden H. Rapid initial reduction of hyperenhanced myocardium after reperfused first myocardial infarction suggests recovery of the peri-infarction zone: one-year follow-up by MRI. *Circ Cardiovasc Imaging*, 2(1): 47-55, 2009.
- [92] Prasad A, Gersh BJ, Bertrand ME, Lincoff AM, Moses JW, Ohman EM, White HD, Pocock SJ, McLaurin BT, et al. Prognostic significance of periprocedural versus spontaneously occurring myocardial infarction after percutaneous coronary intervention in patients with acute coronary syndromes: an analysis from the ACUTY (Acute Catheterization and Urgent Intervention Triage Strategy) trial. *J Am Coll Cardiol*, 54(5): 477-486, 2009.
- [93] Eitel I, Desch S, Fuernau G, Hildebrand L, Gutberlet M, Schuler G, Thiele H. Prognostic significance and determinants of myocardial salvage assessed by cardiovascular magnetic resonance in acute reperfused myocardial infarction. *J Am Coll Cardiol*, 55(22): 2470-2479, 2010.
- [94] Larose E, Rodes-Cabau J, Pibarot P, Rinfret S, Proulx G, Nguyen CM, Dery JP, Gleeton O, Roy L, et al. Predicting late myocardial recovery and outcomes in the early hours of ST-segment elevation myocardial infarction traditional measures compared with microvascular obstruction, salvaged myocardium, and necrosis characteristics by cardiovascular magnetic resonance. *J Am Coll Cardiol*, 55(22): 2459-2469, 2010.

- [95] Caravan P. Strategies for increasing the sensitivity of gadolinium based MRI contrast agents. *Chem Soc Rev*, 35(6): 512-523, 2006.
- [96] Kellman P, Aletras AH, Mancini C, McVeigh ER, Arai AE. T2-prepared SSFP improves diagnostic confidence in edema imaging in acute myocardial infarction compared to turbo spin echo. *Magn Reson Med*, 57(5): 891-897, 2007.
- [97] Messroghli DR, Walters K, Plein S, Sparrow P, Friedrich MG, Ridgway JP, Sivananthan MU. Myocardial T1 mapping: application to patients with acute and chronic myocardial infarction. *Magn Reson Med*, 58(1): 34-40, 2007.
- [98] Green JD, Clarke JR, Flewitt JA, Friedrich MG. Single-shot steady-state free precession can detect myocardial edema in patients: a feasibility study. *J Magn Reson Imaging*, 30(3): 690-695, 2009.
- [99] Sorensson P, Heiberg E, Saleh N, Bouvier F, Caidahl K, Tornvall P, Ryden L, Pernow J, Arheden H. Assessment of myocardium at risk with contrast enhanced steady-state free precession cine cardiovascular magnetic resonance compared to single-photon emission computed tomography. *J Cardiovasc Magn Reson*, 12(1): 25, 2010.
- [100] Diesbourg LD, Prato FS, Wisenberg G, Drost DJ, Marshall TP, Carroll SE, O'Neill B. Quantification of myocardial blood flow and extracellular volumes using a bolus injection of Gd-DTPA: kinetic modeling in canine ischemic disease. *Magn Reson Med*, 23(2): 239-253, 1992.
- [101] Saeed M, Wendland MF, Masui T, Higgins CB. Reperfused myocardial infarctions on T1- and susceptibility-enhanced MRI: evidence for loss of compartmentalization of contrast media. *Magn Reson Med*, 31(1): 31-39, 1994.
- [102] Abdel-Aty H, Simonetti O, Friedrich MG. T2-weighted cardiovascular magnetic resonance imaging. *J Magn Reson Imaging*, 26(3): 452-459, 2007.
- [103] Keegan J, Gatehouse PD, Prasad SK, Firmin DN. Improved turbo spin-echo imaging of the heart with motion-tracking. *J Magn Reson Imaging*, 24(3): 563-570, 2006.
- [104] Judd RM, Lugo-Olivieri CH, Arai M, Kondo T, Croisille P, Lima JA, Mohan V, Becker LC, Zerhouni EA. Physiological basis of myocardial contrast enhancement in fast magnetic resonance images of 2-day-old reperfused canine infarcts. *Circulation*, 92(7): 1902-1910, 1995.
- [105] Lima JA, Judd RM, Bazille A, Schulman SP, Atalar E, Zerhouni EA. Regional heterogeneity of human myocardial infarcts demonstrated by contrast-enhanced MRI. Potential mechanisms. *Circulation*, 92(5): 1117-1125, 1995.
- [106] Peshock RM, Malloy CR, Buja LM, Nunnally RL, Parkey RW, Willerson JT. Magnetic resonance imaging of acute myocardial infarction: gadolinium

diethylenetriamine pentaacetic acid as a marker of reperfusion. *Circulation*, 74(6): 1434-1440, 1986.

- [107] Wesbey GE, Higgins CB, McNamara MT, Engelstad BL, Lipton MJ, Sievers R, Ehman RL, Lovin J, Brasch RC. Effect of gadolinium-DTPA on the magnetic relaxation times of normal and infarcted myocardium. *Radiology*, 153(1): 165-169, 1984.
- [108] Kim RJ, Chen EL, Lima JA, Judd RM. Myocardial Gd-DTPA kinetics determine MRI contrast enhancement and reflect the extent and severity of myocardial injury after acute reperfused infarction. *Circulation*, 94(12): 3318-3326, 1996.

Acknowledgments

This thesis would never have been possible without the contribution, support and help from many people. I wish to express my appreciation to all of you and my special gratitude to:

My supervisor, **Håkan Arheden**, for inviting me to Sweden and accepting the heavy burden of guiding and supporting me through this PhD program. Thank you for your excellent guidance, thoughts about leadership and communication, and for teaching me about patience.

My co-supervisor, **Henrik Engblom**, for great discussions, teaching me scientific writing and most of all, for your inspirational work ethics.

Galen Wagner, for introducing me to the world of research. Your overwhelming enthusiasm and optimism for research stimulated me to pursue a PhD when I was still a medical student.

Marcus Carlsson, for letting me work clinically, ‘forcing’ me to speak Swedish, and for challenging me with new insights to discussions.

Mikael Kanski, for friendship, companionship during late night experiments and for being a great colleague.

To all my colleagues in the Cardiac MR Group and at the Department of Clinical Physiology, for friendship, support and for teaching me new things every day: **Olle Pahlm, Einar Heiberg, Martin Ugander, Erik Hedström, Helen Soneson, David Strauss, Johannes Töger, Jane Sjögren, Katarina Steding, Karin Markenroth Bloch, Sverrir Stephensen, Robert Jablonowski, Jonas Jögi, Bo Hedén, Henrik Mosén, Ann-Helén Arvidsson, Christel Carlander, Johanna Carlson and Lotta Åkesson.**

Kerstin Brauer, Karin Larsson and Märta Granbohm for all help with teaching and administrative work.

This thesis would not be possible without the unlimited support from my colleagues at the Department of Cardiology: **David Erlinge, Stefan Jovinge, Sasha Koul, Jesper van der Pals, Matthias Göteborg and Patrik Andersson.** Thank you for stimulating discussions and our fruitful collaborations. A particular thanks goes to Sasha for being a great friend and teaching me ‘your’ part of the experiments.

All my friends in the Netherlands, who despite me being in Sweden, still welcomed me with open arms whenever I returned to the Netherlands for a short ‘holiday’.

My wonderful parents, **Will** and **Miriam**, and my sister **Kim**, for all your love and support through my life, for always believing in me and for coping with my travels. Words can not describe my gratitude! Your morals and standards made me the person I am today.

My godparents, **John** and **Marlies**, for support and for being the best godfather and godmother one could possibly have.

Finally, **Yvette**, for your unconditional love and support in every aspect, and for companionship, understanding and endurance.

Studies I - IV